Check for updates

Progress on the luminescence mechanism and application of carbon quantum dots based on biomass synthesis

Lei Wang, [ID] Shujia Weng, [ID] Shuai Su [ID] and Weiwei Wang [ID] *

With the continuous development of carbon-based materials, a variety of new materials have emerged one after another. Carbon Quantum Dots (CQDs) have succeeded in standing out from the crowd of new materials due to their better optical properties in biomedicine, ion detection, anti-counterfeiting materials and photocatalysis. In recent years, through the continuous exploration of CQDs, research scholars have found that the organic substances or heavy metals contained in traditional ones can cause irreversible harm to people and the environment. Therefore, the application of traditional CQDs in future studies will be gradually limited. Among various new materials, biomass raw materials have the merits of good biocompatibility, lower toxicity and green and environmental protection, which largely overcome the defects of traditional materials and have attracted many scholars to focus on the research and development of various biomass CQDs. This paper summarises the optical properties, fluorescence mechanisms, synthetic methods, functionalisation modulation of biomass CQDs and their relevant research progress in the fields of ion detection, bioimaging, biomedicine, biosensing, solar cells, anti-counterfeit materials, photocatalysis and capacitors. Finally, the paper concludes with some discussion of the challenges and prospects of this exciting and promising field of application.

Introduction

With their unique properties, C-based nanomaterials have played important roles in recent years in scientific and technological research and development.[1–3] Among them, nanodiamonds, fullerenes, C-nanotubes, graphene, and fluorescent C-nanoparticles have become the most researched class of

School of Life Science and Chemistry, MinNan Science and Technology University, Quanzhou 362332, China. E-mail: wangweiwei@mku.edu.cn; 122572020058@mku.edu.cn

materials in nanotechnology.[4–8] Their great potential to be used in a wide range of applications has greatly stimulated the interest of researchers and scholars and driven them to actively engage in the research of C-based nanomaterials.[9–11] In the past few years, C-nanoparticles and semiconductor materials have been successfully used in a variety of applications such as bioimaging, biosensing and medical diagnostics due to their strong, tunable fluorescence emission properties. However, these materials have certain limitations, such as the use of many toxic reagents, such as pyridine,[12] pyrrole,[13] and heavy metal salts,[14] in the preparation of these materials *etc*. It is well

Lei Wang was born in China in 2002. He is currently studying at Minnan University of Science and Technology, where he has joined the subject group and started his research career. His research interests are mainly focused on the exploration of synthetic methods, optical properties and application prospects of nanomaterials. So far, he has published several relevant research papers.

Weiwei Wang received her PhD from Dalian University of Technology, China in 2020. She joined Minnan Science and Technology University, China in 2020 as a associate professor. Her research interests focus on the design and construction of nanocatalysts and CO_2 utilization. She has published more than 15 peer reviewed journal papers as the first author or corresponding author.

known that these reagents are not only cumbersome to handle and require specific safety precautions, but also produce high levels of reproductive toxicity, neurotoxicity, *etc.*, even at relatively low levels, which will hinder the practical application of carbon nanoparticles and semiconductor materials in clinical medicine, bioimaging and other fields. These reasons lead to the creation of (Carbon Quantum Dots, CQDs). CQDs are new sphere-like carbon nanoparticles in the size range 1–10 nm, which have excellent optical and electrical properties, stability and low toxicity, and are therefore increasingly being used to replace fluorescent nanomaterial particles and semiconductor materials.

CQDs are usually carbon nanomaterials consisting of sp^2/sp^3 carbon cores and external oxygen/nitrogen-containing functional groups. They consist of monodisperse spheres less than 10 nm in size.[15,16] CQDs not only have better biocompatibility, excellent fluorescence quantum yields, and coordinable photoluminescence (PL) properties, but also their low cost and low toxicity. In 2004, CQDs were discovered by chance as a by-product in monolayer carbon nanotubes prepared by arc discharge method.[17] In 2006, Sun[18] prepared fluorescent CQDs with tunable visible wavelengths by laser cautery. Since then, a large number of scientific researchers and scholars have started to research and explore CQDs continuously, and they have used many different types of carbon source precursors (such as small molecule organic compounds, carbon fiber materials, biomass-based materials, *etc.*) to synthesize CQDs by various methods such as pyrolytic carbonization, hydrothermal method, microwave method, electrochemical oxidation method, and combustion method.[170]

Currently, a large number of researchers have now started to use biomass materials widely available in nature. They have successfully prepared biomass-based CQDs using materials such as fish scales,[19] peanuts,[20] holy basil,[21] sweet potato peels,[22] tea leaves,[23] mangoes,[24] caffeine,[25] lignin,[26] starch[27] and soybeans[28] as the initial carbon source. The use of biomass-based preparation of CQDs can not only reduce the cost of raw materials in the preparation process and realize the multiple recycling of waste resources, but also the CQDs prepared in this way usually have very excellent biocompatibility and good fluorescence emission properties, and can directly select green and pure natural precursors from the source, which greatly improves the feasibility of green environmental protection. Therefore, CQDs prepared using biomass-based can be more effectively and safely used in medical diagnostic fields such as bioimaging and biosensing.[29] In addition, it can effectively solve the problem of poor photostability of traditional fluorescent dyes and is expected to be an alternative to medical materials prepared from traditional fluorescent dyes, fluorescent nanoparticle materials, and semiconductor materials.[30–32]

To this end, this paper systematically analyses the research progress of biomass CQDs, focusing on three aspects: firstly, the optical properties of biomass CQDs, secondly, the fluorescence mechanism of biomass CQDs, and thirdly, the study of how to design, prepare and modulate biomass CQDs with excellent optical properties using biomass materials as the initial carbon source. On this basis, it also introduces the application of biomass CQDs in ion detection, bioimaging, biomedicine, biosensing, solar cells, anti-counterfeiting materials, catalysis, capacitors and other related applications. It is hoped that this paper will provide the most comprehensive analysis possible of the research progress in the development of biomass CQDs for the general research community. It will provide some theoretical basis for further research by scholars in the future.

Optical properties of biomass CQDs

CQDs have achieved many excellent physical and chemical properties due to their unique chemical structure, the most prominent of which are optical properties, mainly including UV visible absorption characteristics, fluorescence characteristics, fluorescence stability, and so on. Researchers have compared biomass CQDs with traditional semiconductor quantum dots, metal CQDs, and CQDs synthesized with organic reagents, and found that the optical properties of biomass CQDs are similar to or even better than semiconductor CQDs, metal CQDs, and CQDs synthesized with organic reagents. As a result, biomass CQDs have attracted the attention of many scholars. Therefore, biomass CQDs has attracted the attention of many scholars. In this section, we will introduce the optical properties of biomass CQDs and their related calculations.

UV-vis absorption properties

CQDs usually have strong light absorption in the ultraviolet region and weak light absorption intensity in the visible and near-infrared regions,[33] but a small part of CQDs also have strong light absorption peaks in the visible region.[34,35] Usually, the absorption peaks of biomass CQDs are mainly located between 230–270 nm and 320–380 nm. The absorption peaks between 230–270 nm are due to π–π^* transitions in sp^2 hybrid carbon, while the absorption peaks between 320–380 nm are due to n–π^* transitions in C=O,[36–38] as shown in Fig. 1(a). Lee[39] *et al.* synthesized a nitrogen doped biomass CQDs with bright blue fluorescence using plum fruit as the reaction raw material through a one-step hydrothermal method. As shown in Fig. 1(b), the absorption peaks of the CQDs are 270 nm and 332 nm, which belong to the π–π^* transition of C=C and n–π^* transition of C=O, respectively. In addition, according to relevant research reports, we found that after the heteroatomic doping and surface functionalization modification of CQDs, its absorption ability, emission wavelength and peak intensity of visible light would be greatly changed,[40] which greatly changed the optical properties of CQDs. Wang[41] *et al.* successfully introduced an amino structure in the preparation of CQDs, as shown in Fig. 1(c). It can be seen that the amino structure can significantly improve the visible light absorption ability of CQDs. Sun[40] *et al.* successfully prepared S–N–S-CQDs by carbonizing with sulfuric acid using hair fiber as carbon source. In this experiment, different temperature gradients were set for the synthesis reaction. As shown in Fig. 1(d) and (e), we can observe that with the continuous increase of temperature, the S element in CQDs gradually increases, and the absorption peak of the CQDs undergoes a blue shift, with a peak change of
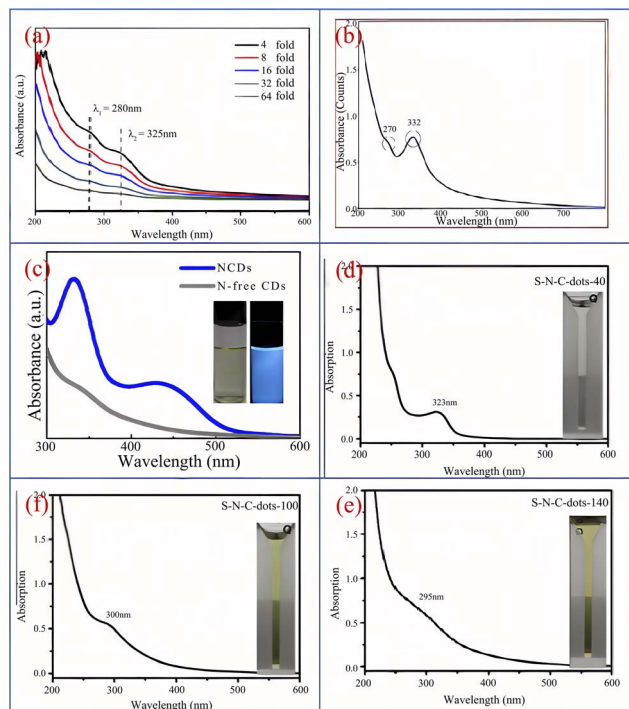
Fig. 1 (a) UV-vis spectra of biomass CQDs at different dilution ratios;[36] (b) UV-vis spectra of N-CQDs;[39] (c) UV-vis spectra of N-CQDs and N doped CQDs;[41] (d, e and f) the UV-vis spectrogram presented with the continuous increase of S element in CQDs.[40] Reproduced from ref. 36 with permission from [Elsevier], copyright [2023]. "Reproduced from ref. 39 with permission from [Elsevier], copyright [2023]". "Reproduced from ref. 41 with permission from [Springer], copyright [2023]". "Reproduced from ref. 40 with permission from [Elsevier], copyright [2023]".

323 nm → 300 nm → 295 nm, but the emission peak gradually undergoes a red shift. In addition, there are also some CQDs emitted in the near-infrared light region, usually because sp² carbon atoms and their surface groups contain π electrons, which will produce π conjugated effect, resulting in their long wavelength light absorption in the range of 500–800 nm.[42] Therefore, the differences in chemical composition, structure, preparation process, modification and modification methods of biomass CQDs can lead to changes in UV-vis.

Fluorescence characteristics

Photoluminescence refers to the phenomenon that a material is irradiated by an external light source and thus excited to produce light emission.

Photoluminescence is one of the outstanding properties of CQDs. Due to the differences in preparation methods, raw materials, reaction conditions and pH, the fluorescence characteristics of CQDs are significantly different, so that the emission spectrum of CQDs covers the whole light absorption region. The photoluminescence behavior of CQDs is usually divided into two processes: excitation and emission. It is worth noting that both processes originate from a jump between different energy levels.

Song[37] et al. synthesized CQDs with bright blue fluorescence by one-step hydrothermal method using black tea as raw
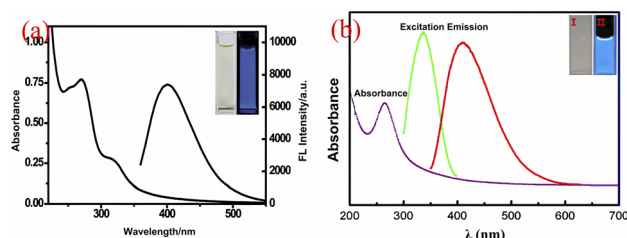

Fig. 2 (a) UV-vis absorption and emission spectra of CQDs under 320 nm excitation;[37] (b) fluorescence emission and UV-vis absorption spectra of CQDs, as well as images of CQDs under sunlight and ultraviolet lamp irradiation.[43] "Reproduced from ref. 37 with permission from [Royal Society of Chemistry], copyright [2023]". "Reproduced from ref. 43 with permission from [Elsevier], copyright [2023]".

material. As shown in Fig. 2(a), under the excitation of 320 nm ultraviolet irradiation light, the optimal emission peak is 400 nm. When the wavelength of the ultraviolet irradiation light is constantly changed, we can observe that the peak position and intensity of the emission peak also change accordingly. Yang[43] et al. successfully prepared CQDs using honey as a carbon source. As shown in Fig. 2(b), the CQDs emitted bright blue fluorescence upon irradiation with UV light at 365 nm, but under daylight conditions, the CQDs showed an almost transparent colour. Furthermore, we can see from the figure that the best excitation and emission wavelengths of this biomass CQDs can be observed at 338 nm and 420 nm respectively. Ding[44] et al. successfully prepared a CQDs with high quantum yield (QY = 28%) and red light emission by solvothermal method using lemon juice as raw material, and its optimal emission wavelength is 631 nm. In addition, scholars have found that acidity and alkalinity also have a significant impact on the photoluminescence of CQDs. Chunduri[45] et al. successfully prepared CQDs with a large amount of carboxyl and amino groups on the surface using coconut shell. After continuous testing, we found that the fluorescence of CQDs gradually decreased when pH increased from 4 to 12. This is mainly because the carboxyl group will undergo protonation and deprotonation under different PH conditions, which will cause the change of electrostatic charge, and then cause the change of fluorescence. Jia[46] et al. found that the emission intensity of CQDs prepared using ascorbic acid as a carbon source exhibits a linear relationship between pH 4–8. When pH > 8, the emission intensity decreases by up to 90% compared to pH = 4. This may be due to the deprotonation of carboxyl groups on the surface of CQDs caused by the rise in pH. In addition, some CQDs have the highest emission intensity at pH = 7, while in acidic or alkaline environments, their emission intensity will significantly decrease.[47] In addition, stable PL emission over a wide range of ionic strengths is important for the practical application of carbon quantum dots (CQDs), mainly because variations in ionic strength affect the charge density and surface reactivity of the surface of CQDs, which in turn affects their fluorescence emission properties. If the emission of CQDs is unstable, it will affect the effectiveness of their specific applications in bioimaging, optoelectronics, sensors and other fields.
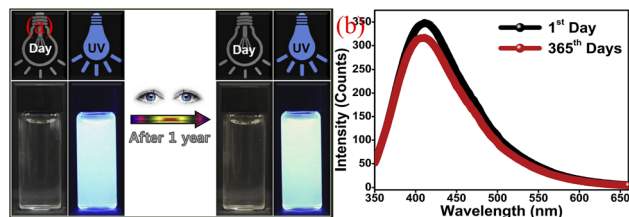
Fig. 3 Comparison of fluorescence spectra (a) and fluorescence emission spectra (b) of CQDs prepared from apple juice stored for 1 day and 365 days, respectively.[50] "Reproduced from ref. 50 with permission from [Elsevier], copyright [2023]".

Optical stability

Another advantage of CQDs is that it has good fluorescence stability.[48] The fluorescence intensity of traditional organic dyes or dyes usually decreases rapidly with the increase of light, while the fluorescence intensity of CQDs hardly weakens under continuous ultraviolet irradiation, and it also has extremely strong photobleaching resistance.

Sun[18] et al. subjected the synthesized CQDs to several successive repeated excitations, and they found that their fluorescence intensity did not show any decay and the fluorescence emission of the CQDs did not show light flicker under confocal microscopy. Li[49] et al. subjected CQDs made by laser stripping to continuous UV light irradiation for 4 h and found that the fluorescence intensity of CQDs decreased by only 4.5%. Lee[50] research group used apple juice as the precursor to synthesize biomass CQDs with high quantum yield (QY = 12.5%) and bright blue fluorescence by one-step hydrothermal method. As shown in Fig. 3, the research group stored the CQDs for 365 days, and then compared them with the first day. They found that a storage time of up to 365 days did not significantly change the fluorescence emission intensity of the CQDs, only slightly attenuated.

Therefore, based on the stable and excellent fluorescence stability of CQDs, people can make full use of these characteristics and better apply them in various fields such as *in vivo* labeling and detection, imaging and so on. We believe that in the near future, we can see a large area of practical application of CQDs, bringing more convenience to human beings.

Calculation of relative fluorescence quantum yields

Fluorescence quantum yield (QY) is the ratio of the number of fluorescent photons emitted by a fluorescent substance after it absorbs light to the number of photons absorbed by the excited light. The larger the QY of the fluorescent material is, the higher the fluorescence intensity is, and the smaller it is, the lower the fluorescence intensity is. In any case, the quantum yield of the fluorescent material will not exceed 1. If the material has no fluorescence emission, its quantum yield will be equal to or infinitely close to 0. Since the absolute accurate QY value is difficult to measure, the reference method is usually used to measure it.

At present, the most commonly used method is quinine sulfate as a ref. 51. The specific methods are as follows: firstly, a certain amount of quinine sulfate (QY = 54%, $\eta = 1.33$) is dissolved in 0.1 M H_2SO_4 solution, and then a series of standard reference solutions with different concentration gradients are configured.

Secondly, dissolve the required measured CQDs in deionized water and prepare a series of corresponding CQDs to be tested solutions. Thirdly, adjust the concentration of the standard reference solution and the sample solution to be tested to ensure that their absorbance at 360 nm can be less than 0.1, preferably close to 0.05. Finally, the absorbance values at the wavelength of 360 nm are obtained respectively, then the fluorescence emission peaks of the reference solution and the sample to be measured are scanned at the excitation wavelength of 360 nm, the area is calculated, and the value is brought into the following formula to calculate the fluorescence quantum yield:

$$Y_S = Y_R \times \frac{I_S}{I_R} \times \frac{A_R}{A_S} \times \frac{\eta_S^2}{\eta_R^2}$$

In the formula, Y represents the fluorescence quantum yield; I is the area of the fluorescence emission peak; A is the absorbance value of the solution at 360 nm; η indicates the refractive index of the solution; the subscripts S and R represent the solution to be tested and the quinine sulfate standard reference solution, respectively.

Calculation of average fluorescence life

The average lifetime of fluorescence refers to the average duration of fluorescence emitted by a substance after absorbing energy under the action of an excited light source. The average lifetime of fluorescence is an extremely important index parameter, which is often used to describe the fluorescence characteristics of fluorescent materials. It can well reflect the fluorescence decay rate and internal energy transfer process of fluorescent materials. Therefore, it can be widely used in materials chemistry, biomedicine, physical chemistry and other fields.

Similarly, the fluorescence average lifetime index also plays a crucial role in the optical properties of CQDs. It can well reflect the temporal variation of the fluorescence signal of CQDs and the magnitude of the change in fluorescence decay rate. The decay rate of fluorescence signals is inversely proportional to the average fluorescence lifetime. Generally, the longer the average fluorescence lifetime, the slower the signal decay rate changes. If the duration is longer, the stronger its fluorescence stability and reliability.

The following equation is the average fluorescence lifetime equation:[52]

$$\tau_{av} = a_1\tau_1 + a_2\tau_2 + a_3\tau_3$$

Among them, τ_1, τ_2, τ_3 represents the decay time of each part of CQDs, and a_1, a_2, and a_3 represent the corresponding weights of each part of CQDs.

Fluorescence mechanism of biomass CQDs

The luminescence mechanism of CQDs is closely related to their synthesis process. As different biomass CQDs are prepared from different raw materials, synthesis methods and pre-

treatment processes, the chemical structures and compositions of the synthesised CQDs are usually different, which also leads to different optical properties. This has attracted many researchers and scholars to investigate the luminescence mechanism of CQDs, but there is still a great deal of controversy among them. Currently, the most recognised fluorescence mechanisms for CQDs are the following: band gap fluorescence from band gap jumps in conjugated π-domain structures, surface state luminescence, molecular state luminescence, down-conversion luminescence, and up-conversion luminescence.

Bandgap fluorescence from bandgap jumping in conjugated π-domain structures

For some CQDs with graphitized structures, their fluorescence effect is inextricably linked to the π-electron state of the sp^2 structure. The band gap of the conjugated π-domain structure leaps to produce band gap fluorescence, with the band gap leap occurring mainly in the π-structure domain. They are like isolated islands in which are rich in π-electrons and have sp^2 hybridization, and these islands can be formed by reducing the graphene oxide. If multiple islands are joined together. Then it will happen sudden fluorescence extinction.[53] Therefore, to avoid sudden fluorescence extinction, we should isolate the π-structural domains from each other, which will facilitate the formation of band-gap fluorescence. In addition, a monolayer of graphene sheets must be used to isolate it. This prevents interlayer occurrence in multilayer graphene sudden extinction.[54]

In addition to this, the fluorescence emission for graphitized structured CQDs can also be tuned by changing the size of the conjugated π-domain. As the conjugate π-domain shrinks, the size of the carbon nuclei of CQDs also becomes progressively smaller, fluorescence emission and UV absorption shifts in the direction of blue shift; conversely, the size of the carbon cores of CQDs also gradually increases, fluorescence emission and UV absorption shifts in the direction of red shift. This explains well the luminescence mechanism of the graphitized structures of CQDs.

Surface state luminescence

The surface state of CQDs (chemical groups, degree of oxidation of the surface, surface defects) is closely related to the fluorescence emission of CQDs. The use of multiple methods for the synthesis of CQDs has resulted in very complex chemical structures on the surface of CQDs, such as different hybridised carbon atoms, surface defects and various functional group structures.[55–58] As shown by Fig. 4, the fluorescence emission of CQDs is related to the degree of oxidation of the surface, and an increase in the oxidation of its surface shifts the fluorescence emission of CQDs towards the red-shift direction. This is because surface oxidation introduces surface defects to CQDs, and different defects introduce a variety of fluorescent emission sites on CQDs, so their emission spectral intensity will change, and when the surface oxidation of CQDs is higher, more surface defects will be introduced, which will capture more excitons for
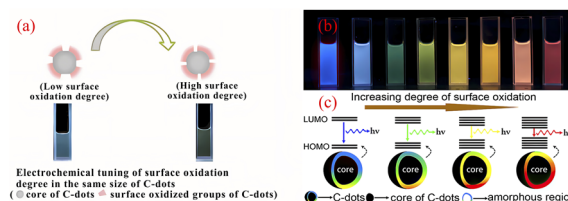

Fig. 4 (a) Effect of different levels of surface oxidation on the fluorescence of CQDs;[59] (b) fluorescence plots of CQDs with different levels of oxidation under UV light irradiation;[58] (c) fluorescence modulation mechanism of CQDs with different oxidation levels.[58] "Reproduced from ref. 59 with permission from [John Wiley and Sons], copyright [2023]". "Reproduced from ref. 58 with permission from [American Chemical Society], copyright [2023]".

compounding to produce radiation, thus causing the spectral emission to shift in the red-shifted direction,[59] and the different luminescent colours are mainly related to the surface oxidation and surface structure of the CQDs, independent of the particle size.[58]

In addition, the graphite powder was laser ablated to obtain non-fluorescent effect CQDs, subsequent oxidation of the CQDs by UV light produced oxygen-containing groups on their surface. With the increase in the number of oxygen-containing groups, CQDs succeeded in possessing fluorescence emission properties, thus demonstrating that the source of fluorescence for CQDs comes from the surface state structure, independent of the size of the carbon nucleus and the size of the energy gap in the surface state.[60] Some studies have also shown that when CQDs have the same particle size and similar surface oxygen content, the fluorescence gradually redshifts as the number of amide groups increases. This is because the N-containing electron donating groups, which causes a substantial enhancement of the n–π* leap, and the width of the energy gap narrows as the number of N-containing groups increases, leading to its enhanced fluorescence emission capacity, eventual fluorescence occurs red shift.[61]

Molecular state luminescence

The luminescence mechanism of the molecular state differs from that of the previous two. Many studies have shown that a number of small fluorescent molecules or fluorophores are produced during the synthesis of CQDs and that, as the reaction continues, they are eventually complexed to the surface of the CQDs or embedded within it, making the CQDs fluorescent.[62] As shown in Fig. 5, comparing the CQDs synthesised from three raw materials – citric acid and ethylenediamine, citric acid and hexamethylenetetramine, and citric acid and triethanolamine – with citrazinic acid, it can be concluded that the fluorescence of the CQDs synthesised from the first two raw materials, which emit bright blue fluorescence, originates from the citrazinic acid molecules modified on their surfaces.[63]

Some other studies have also found, at low temperatures, as the reaction continues, will form molecular precursors with fluorescent groups, the fluorescence at this time is mainly molecular fluorescence; as the reaction temperature gradually
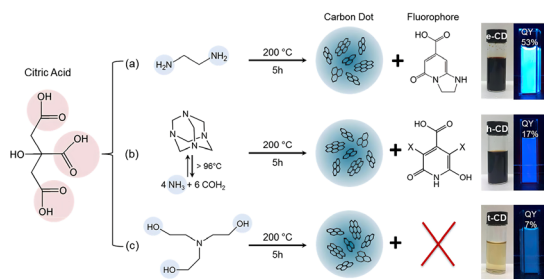
Fig. 5 Reaction conditions for the synthesis of citric acid-based CQDs using three different raw materials and the corresponding images under ambient and UV light irradiation.[63] "Reproduced from ref. 63 with permission from [American Chemical Society], copyright [2023]".
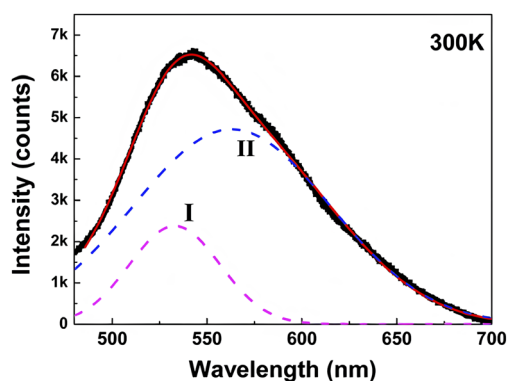

Fig. 6 Fitting of fluorescence spectra of CQDs.[66] "Reproduced from ref. 66 with permission from [American Chemical Society], copyright [2023]".

increases, the fluorescent group is present alongside the cross-linked polymer, at which point the fluorescence emission is thought to be provided by both the carbon nucleus and the fluorescent group; as the temperature continues to rise, the size of the carbon nuclei of CQDs increases and the fluorescent groups gradually decrease, at which point the fluorescence emission is then thought to originate mainly from the carbon nuclei.[64,65] The same conclusion was reached by Yu[66] et al. when they explored the effect of temperature on the fluorescence of CQDs, as can be seen through Fig. 6 that the fluorescence luminescence of CQDs is the result of the combined effect of both carbon core luminescence and fluorescent group luminescence.

Down-conversion luminescence

Down-conversion luminescence is a photoluminescence phenomenon in which a material emits two or more low-energy photons when excited by a short-wavelength light wave with high energy. In CQDs, the behaviour of down-conversion luminescence is mainly characterised by wavelength-coordinated emission.

At present, Sun,[67] Qu,[68] Kailasa,[69] Bhamore[30] have successfully prepared wavelength coordinated emission CQDs using artificially synthesized carbon sources. They

exhibit emission of multiple fluorescent colors,[18] as shown in Fig. 7(a). Related researchers believe that the wavelength coordinated emission of CQDs is mainly related to their surface defects and particle size.[70] Therefore, we can achieve fluorescence emission of multiple colors of CQDs by introducing more defect states on their surfaces to enable a large number of excitons to recombine, or by adjusting the size of the particle size. In recent years, the technology of synthesizing CQDs with synthetic carbon source for wavelength coordinated emission has been relatively mature, while the technology of synthesizing CQDs with biomass carbon source for wavelength coordinated emission is still in the initial stage. At present, most CQDs produced from biomass raw materials usually emit blue fluorescence, while only a few biomass CQDs emitting red,[71] yellow[72] and green[73] have been reported. Zhou[71] et al. successfully prepared biomass CQDs with four different fluorescence emissions using food waste. They successfully separated four different fluorescent colors of biomass CQDs prepared by hydrothermal carbonization through dialysis. As shown in Fig. 7(b), they are blue (molecular weight <500 Da, QY = 28%), green (molecular weight 500–1000 Da, QY = 18%), yellow (molecular weight 1000–2000 Da, QY = 10%), and red (molecular weight >2000 Da, QY = 6%). It can be found that the continuous increase of particle size will lead to the gradual red shift of fluorescence color, while the continuous increase of molecular weight will cause the dialysis effect to become worse and worse, and the yield of the obtained CQDs will also decrease sharply. Ding[44] et al. successfully prepared a biomass CQDs capable of emitting red fluorescence using lemon juice as a precursor. In order to investigate the effect of the chemical structure on wavelength coordinated emission on the surface of CQDs, researchers used NaBH4 to reduce the chemical structure on its surface. Subsequently, it was found that the red luminescence of the biomass CQDs decreased and
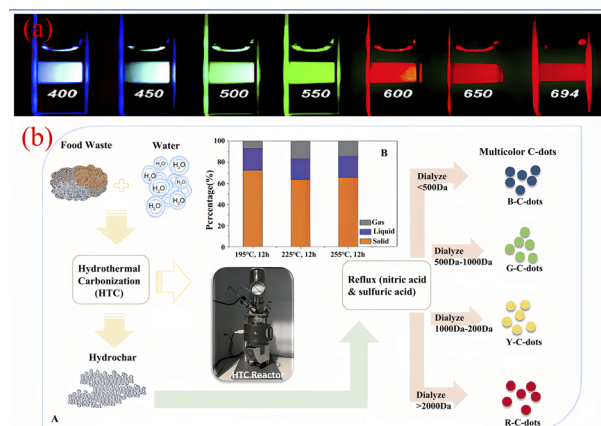

Fig. 7 (a) Fluorescence diagram of CQDs emitted at different excitation wavelengths;[18] (b) preparation process of biomass CQDs with multiple fluorescence emission.[71] "Reproduced from ref. 18 with permission from [American Chemical Society], copyright [2023]". "Reproduced from ref. 71 with permission from [Royal Society of Chemistry], copyright [2023]".

gradually blue shifted emission occurred. Therefore, by modifying and adjusting the surface state of CQDs, a significant change in their fluorescence color can be achieved.

Upconversion luminescence

In addition to down-conversion luminescence, CQDs sometimes exhibit up-conversion luminescence. Upconversion luminescence is an optical phenomenon in which the wavelength of fluorescence emission is less than the excitation wavelength used.[74] Due to the ability of long excitation wavelengths to penetrate deep biological tissues well, as well as their high spatial resolution and low background interference, they play a crucial role in biological imaging. Cao[75] *et al.* first discovered that CQDs has upconversion luminescence property. They observed that CQDs emits visible light under excitation light of 800 nm. However, there are still some controversies about the formation mechanism of upconversion luminescence properties of biomass CQDs. One explanation is the electron relaxation phenomenon of high energy state π orbital transition to σ orbital in biomass CQDs. Another explanation is that biomass CQDs has a huge multi-photon absorption cross section. When it is excited, it can simultaneously absorb multiple long-wave photons and release a short-wave photon, so the emission wavelength is smaller than the excitation wavelength.

Yin[76] *et al.* successfully prepared a biomass CQDs with both down conversion fluorescence and up conversion fluorescence using chili peppers as precursors. After research, it was found that the upconversion fluorescence emission of this CQDs also exhibits excitation wavelength dependence, as shown in Fig. 8(a). Jiang[77] *et al.* prepared a biomass CQDs with upconversion fluorescence using coffee as raw material. The mechanism of upconversion fluorescence of CQDs in biomass may be due to the simultaneous absorption of two or more photons by CQDs, leading to anti-Stokes emission. S–N-CQDs prepared from hair fibers also exhibit upconversion fluorescence properties. As the excitation wavelength increases, the emission wavelength of S–N-CQDs gradually shows a redshift phenomenon.[40] Therefore, multiphoton processes and anti Stokes emission have become the two most recognized mechanisms for the formation of upconversion fluorescence. Due to the relatively low efficiency of upconversion fluorescence, it is usually necessary to adopt high intensity excitation light to

obtain excitation photons or modify or enhance them by some artificial means,[75,78] so as to achieve higher efficiency of upconversion fluorescence.

Synthesis of biomass CQDs

So far, researchers have developed a variety of methods for the preparation of CQDs, as shown in Fig. 9, mainly including two main types of methods, "top-down" and "bottom-up". The "top-down" method involves the complete crushing of the larger carbon skeleton into smaller CQDs by chemical or physical means, mainly including arc discharge, laser pin etching and electrochemical synthesis. The use of the "top-down" method for the preparation of CQDs is usually limited to materials with large sp^2 carbon structural domains. The second major category of "bottom-up" methods refers to the synthesis of larger size CQDs by using small organic molecules as precursors in a series of chemical reactions, mainly including microwave pyrolysis, solvent heat, chemical oxidation, ultrasonic oscillation and hydrothermal methods.

The method described above for the synthesis of CQDs, most of the carbon source precursors they use are non-renewable materials, such as polymeric organic compounds, carbon nanotubes, graphene, organic small molecule compounds, *etc*. These materials are more complex and expensive to handle. What's more, they are toxic, not only does this limit its application in a variety of areas such as bio-imaging, medical therapy and drug delivery, but it also poses a serious and irreversible hazard to people and the environment if improper use results in leakage.

In recent years, China has issued a number of relevant policies to promote high-quality economic development and strengthen environmental protection. The exploration of green technology has become an important engine to promote the development of green economy, which is also one of the reasons for its growing widespread concern. It is for this reason that the synthesis of biomass CQDs has become a major academic hotspot. Biomass materials with a high carbon content and a high abundance of heteroatoms, are a low-cost, green and renewable natural resource. With their good properties, biomass materials have been widely used as precursors to

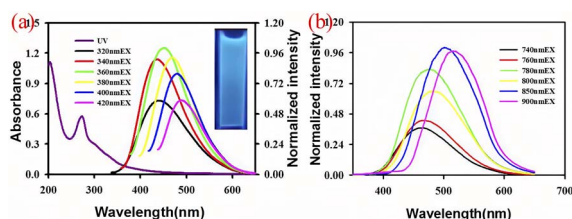**Fig. 8** (a) Fluorescence spectra of biomass CQDs emitted at different excitation wavelengths[76] (b) upconversion fluorescence emission spectra.[76] "Reproduced from ref. 76 with permission from [Royal Society of Chemistry], copyright [2023]".
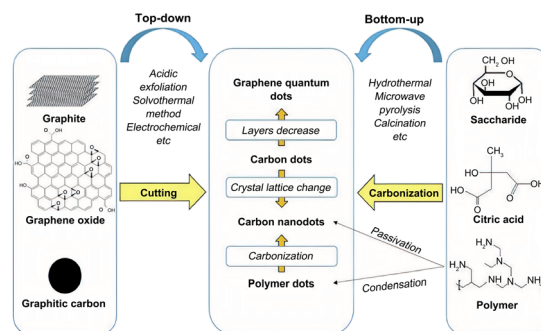

Fig. 9 Introduction to the synthesis method of CQDs.[79] "Reproduced from ref. 79 with permission from [Royal Society of Chemistry], copyright [2023]".

Table 1 Comparison of three CQDs synthesis methods

Synthetic method	Advantage	Disadvantage
Pyrolytic charring method	Simple synthetic process green environmental	The size of the synthesized CQDs is difficult to regulate, the number of surface functional groups is low, and it is difficult to obtain pure CQDs
Microwave method	Efficient and time-saving, high output	Uneven size distribution, high impurities and low quantum yields of prepared CQDs
Hydrothermal method	Wide range of raw materials, green, low cost, easy to realize functionalized modification of CQDs	Long reaction time, low yield, and severe lack of other fluorescent colors

prepare biomass CQDs. CQDs made from biomass materials have excellent luminescence properties, biocompatibility, photostability, low toxicity and many other advantages, this makes it valuable and promising for a wide range of applications in a number of fields such as bioimaging,[80,81] disease treatment,[82,83] catalysis,[84,85] ion detection,[86,87] and optoelectronic devices[88,89] *etc.* In the following, we will briefly describe and introduce these three common current methods for the synthesis of biomass CQDs and discuss their future directions and challenges. The characteristics of the three methods of synthesising CQDs are shown in Table 1.

Pyrolytic charring method

Pyrolytic charring was an early method used to prepare biomass CQDs, mainly under high temperature conditions, using biomass materials as reactants, the degree of pyrolysis and charring is controlled to obtain CQDs with different luminescence properties.

As shown in Fig. 10, Zhou[90] *et al.* used watermelon rind as the raw material and charred the material at 220 °C in air for 2 h. After ultrasonication, centrifugation and dialysis, a biomass CQDs with high fluorescence, water solubility and good fluorescence lifetime was prepared. At the same time, they have also successfully applied it as a fluorescent probe for HeLa cell imaging. Sun[40] *et al.* developed a novel one-step synthesis method for CQDs, a sulphur and nitrogen co-doped S–N-CQDs with good light stability and water solubility was successfully synthesised by the sulphuric acid charring of hair fibres. The researchers added hair fibres to concentrated sulphuric acid and sonicated them at a certain temperature, based on which they were diluted, neutralised, filtered and dialysed, and finally S–N-CQDs were successfully produced.

Yin[76] *et al.* described a simple synthesis of fluorescent CQDs with high sensitivity and both up- and down-conversion. The CQDs were synthesised using bell peppers as precursors. The peppers were first charred at low temperature and then heated in a reactor with water for 5 h, followed by centrifugation and dialysis to obtain purified CQDs. Xue[91] *et al.* used peanut shells as precursors and charred them at 250 °C for 2 h, after cooling, grinding, sonication and filtration, a PH-resistant, strongly fluorescent luminescent and good photobleaching performance CQDs was synthesized. Tan[92] *et al.* prepared CQDs by pyrolysing dried sago waste in a furnace (250–450 °C) for 1 h, followed by cooling, ultrapure water dispersion, sonication and

centrifugation. The CQDs were highly sensitive and were successfully applied to fluorescent probe technology for the detection of metal ions. Ma[93] *et al.* successfully prepared a CQDs with unique excitation-dependent behaviour and good optical properties by putting cleaned peanut shells into a furnace pyrolysis, followed by a series of operations of cooling, grinding, deionised water dispersion, sonication, filtration and permeation.

Microwave method

The microwave method is one of the simplest and most efficient methods for the synthesis of CQDs, and is deeply popular among researchers and scholars. Microwave method refers to

Fig. 10 Schematic diagram of CQDs preparation by pyrolytic carbonization using watermelon rind (a), hair fiber (b), pepper (c), peanut shell (d and f) and sago waste (e) as reaction precursors.[40,76,90–93] "Reproduced from ref. 90 with permission from [Elsevier], copyright [2023]". "Reproduced from ref. 40 with permission from [Elsevier], copyright [2023]". "Reproduced from ref. 76 with permission from [Royal Society of Chemistry], copyright [2023]". "Reproduced from ref. 91 with permission from [Royal Society of Chemistry], copyright [2023]". "Reproduced from ref. 92 with permission from [Elsevier], copyright [2023]". "Reproduced from ref. 93 with permission from [Elsevier], copyright [2023]".

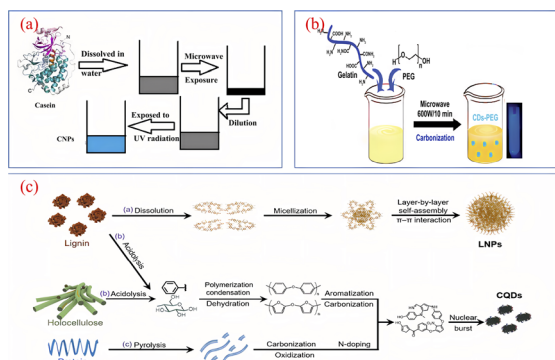**Fig. 11** Schematic diagram of the preparation of CQDs by microwave method using casein (a), gelatin water (b) and air-dried rice straw (c) as reaction precursors.[94,96,98] "Reproduced from ref. 94 with permission from [Springer], copyright [2023]". "Reproduced from ref. 98 with permission from [Taylor & Francis], copyright [2023]". "Reproduced from ref. 96 with permission from [Royal Society of Chemistry], copyright [2023]".

the use of microwave energy under microwave conditions, the uniformity, depth and selectivity of microwave energy, combined with its advantages of rapid and uniform heating to destroy the chemical bonding of the raw material itself, after which it will be dehydrated, polymerised, doped, *etc.*, ultimately forming a method of carbon nanomaterials.

A study of the synthesis of CQDs using the microwave method with biomass as a precursor is shown in Fig. 11. S. K. Bajpai[94] *et al.* prepared a CQDs with blue fluorescence using casein as a raw material by a one-step microwave method, the QY was 18.7% and the synthetic CQDs were applied to leaf cell imaging. Huang[95] *et al.* added *Bauhinia* to a mixture of ethanol and water, which was later placed in a 1000 W microwave apparatus for heating. After cooling, centrifugation, dialysis and freeze-drying, N-CQDs, QY up to 24.0%, were obtained and could be used for Fe^{3+} ion detection with a detection limit of 0.005 μM. Si[96] *et al.* prepared an N-CQDs with purple fluorescence by mixing air-dried rice straw with an aqueous solution of hydrochloric acid and ethanol, followed by a microwave reaction for 10 min, dilution, filtration and centrifugation. Zhao[97] *et al.* used kelp as the main carbon source and reacted it in a (200 °C/800 W) microwave oven for 1.5 h. After cooling down, it was centrifuged, filtered and dialyzed, and a CQDs with high sensitivity to metal ions was successfully produced and applied to metal ion detection. N Arsalani[98] *et al.* prepared bright blue fluorescent CQDs with up to 34.0% QY by using gelatin as the reactant, diluting gelatin into an aqueous solution, adding PEG and mixing it, then heating it in a 600 W microwave oven for 10 min and finally centrifuging it. The anti-tumour efficacy was analysed to be superior to free methotrexate *in vitro* nuclear delivery, which can inhibit tumour growth very efficiently and improve the treatment of cancer in clinical medicine.

Hydrothermal method

The hydrothermal method involves placing the carbon source of the reactants in an autoclave, with water as the solvent, under high temperature and pressure reaction conditions, the process by which small molecular compounds undergo dehydration, polymerisation and charring to form CQDs. The hydrothermal method has the advantages of a simple synthesis process, low cost and controlled conditions. In addition, biomass materials are used as reaction raw materials, which in addition to the basic elements also possess significant amounts of sulphur, nitrogen, *etc.*, during the hydrothermal reaction, the doping element reaction can also take place simultaneously, which gives the CQDs surface a richer functional group structure. Currently, a variety of biomass materials have been prepared by hydrothermal methods for the preparation of CQDs, such as fruits, vegetables, plants and fungi.

As shown in Fig. 12, Wei[99] *et al.* prepared a sulphur and nitrogen co-doped CQDs showing green fluorescence with a QY of 10.48% by a hydrothermal reaction using onions as precursors. First, onion slices were mixed with water and hydrothermally treated at 220 °C for 3 h before being centrifuged, dialyzed and freeze-dried to obtain CQDs, which have good cell penetration and optical selectivity and provide multicolour imaging of intracellular MCF-7 and K562 cells and cytoplasm. Miao[100] *et al.* dissolved tobacco in NaoH solution, diluted it with water and transferred it to an high pressure reactor, where it was hydrothermally treated at 80 °C for 3 h. After a series of operations of cooling, centrifugation, filtration and permeation, a CQDs with blue fluorescence and QY up to 27.9% was produced. Liu[22] *et al.* synthesised CQDs with good photostability and low toxicity from sweet potato peel, which had blue fluorescence and a QY of 8.9%. They mixed sweet potato peel with water in an high pressure reactor and produced pure CQDs by hydrothermal treatment at 200 °C for 3 h followed by filtration and permeation. Wang[101] *et al.* used durian fruit pulp as the raw material, mixed it with water and put it into an high pressure reactor with a platinum sheet at the bottom and hydrothermally treated at 150 °C for 12 h. Finally, ultra-high quantum yield (QY = 79%), sulphur-doped graphene quantum dots (S-GQDs) were successfully obtained. Chellasamy[102] *et al.* used maple leaves as the initial carbon source, mixed with water and stirred, then placed in an autoclave for hydrothermal treatment at 190 °C for 8 h. After completion of the reaction, CQDs

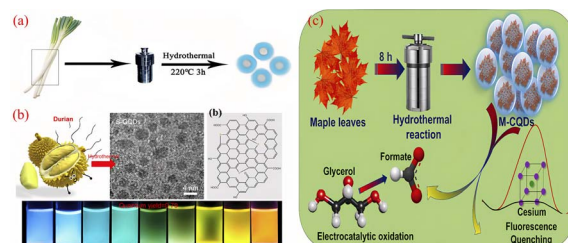**Fig. 12** Schematic diagram of the preparation of CQDs by hydrothermal method using onion (a), durian pulp (b) and maple leaf (c) as reaction precursors.[99,101,102] "Reproduced from ref. 99 with permission from [Royal Society of Chemistry], copyright [2023]". "Reproduced from ref. 101 with permission from [American Chemical Society], copyright [2023]". Reproduced from ref. 102 with permission from [Elsevier], copyright [2023]".

with blue fluorescence were successfully produced through a series of operations such as filtration, centrifugation and filtration.

The synthesis of CQDs by hydrothermal method is simple and easy to achieve functionalized modification and doping of CQDs, which is why the hydrothermal method is favored by many researchers. However, since the reaction temperature and reaction time of the hydrothermal reaction largely determine aspects such as the size, morphology and quantum yield of CQDs, so its fluorescence performance will also be affected to varying degrees.[103,104] For different biomass materials, the optimum temperature and time for their hydrothermal reactions cannot be determined precisely, so a great deal of time and effort is required to try and experiment to determine the optimum temperature and time.

Regulating means of biomass CQDs

As shown in Table 2, the quantum yield of most CQDs made from biomass is generally low without modification; the fluorescence colour of biomass CQDs is single, mostly blue fluorescence, and there is a serious lack of other fluorescence colours, which greatly limits their application in bioimaging; the scope of application of biomass CQDs is limited to bioimaging and sensing. So how to further develop tunable fluorescence CQDs and apply them in deeper fields will be one of the urgent problems to be solved nowadays.

The small particle size and large specific surface area of biomass CQDs lead to the incomplete coordination of their surface, which leads to the formation of a large number of unsaturated bond structures. Under these conditions, the atoms on the surface of biomass CQDs will show higher chemical reactivity, which is easier to complexe with other atoms and groups.[105] In addition, the raw materials for the synthesis of biomass CQDs are all natural organic molecular structures, which makes their surface rich in a large number of functional groups. Therefore, we can effectively control the
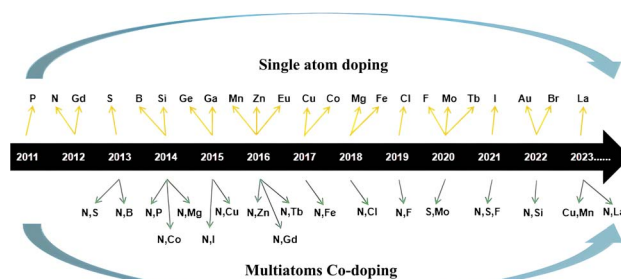

Fig. 13 Time progression table for CQDs doped with different heteroatoms.

fluorescence characteristics and quantum yield of biomass CQDs by modifying their surface. According to research reports, heteroatom doping on the surface of carbon dots[106] and regulating the size distribution of carbon dots[107] are effective ways to improve the fluorescence performance and quantum yield (Fig. 13).

Heteroatomic doping

Miscellaneous atoms are usually divided into non-metallic and metallic atoms. Non-metallic atoms include N, P, S and the halogen group of elements, *etc.*, while metal atoms include Cu, Ge, Gd, *etc.* Currently, the use of heteroatom doping to modulate the fluorescence emission properties and physicochemical properties of CQDs is a very efficient means of doing so. The method focuses on improving the fluorescence properties and quantum yields of CQDs by modulating their chemical structure, carbon skeleton structure, and band gap.[108,109] In addition to the individual doping of metallic and non-metallic atoms, several related studies have reported the modulation of CQDs by multi-element doping.[108] Since metallic atoms are often toxic and can be harmful to humans and the environment, therefore, this section will focus on non-metallic atomic doping and co-doped CQDs.

Table 2 CQDs synthesis summary

Precursor	Synthetic method	Fluorescent color	Quantum yield (%)	Application	Ref.
Watermelon rind	Carbonisation at 300 °C	Blue	7.1	Bioimaging	90
Hair fiber	H_2SO_4 treatment	Blue	11.1	Bioimaging	40
Sweet pepper	Low temperature carbonization	Blue	19.3	ClO^- sensing	76
Peanut shell	Carbonisation at 250 °C	Blue	9.91	Bioimaging	91
Sago scrap	Pyrolytion at 250–450 °C	Blue	—	Metal ion sensing	92
Peanut shell	Pyrolytion at 340–420 °C	Blue	10.58	Cu^{2+} sensing	93
Casein	Microwave treatment	Blue	18.7	Bioimaging	94
Bauhinia	Microwave treatment (1000 W)	Blue	27.0	Fe^{3+} sensing	95
Air-dried straw	Microwave treatment	Purple	—	Bioimaging	96
Kelp	Microwave treatment (800 W)	Blue	23.5	Co^{2+} sensing	97
Gelatin	Microwave treatment (800 W)	Blue	34.0	Drug delivery	98
Onion	Hydrothermal treatment at 140 °C	Green	10.48	Bioimaging	99
Tobacco	Hydrothermal treatment at 140 °C	Blue	27.9	Tetracycline sensing	100
Sweet potato peel	Hydrothermal treatment at 200 °C	Blue	8.9	Oxytetracycline sensing	22
Durian	Hydrothermal treatment at 150 °C	Multiple colors	79.0	Bioimaging	101
Maple leaf	Hydrothermal treatment at 190 °C	Blue	—	Cs sensing	102

Doping of non-metallic atoms

Amongst the many non-metallic atoms, the nitrogen atom is the most commonly doped atom for CQDs.[110] This is due to the fact that the nitrogen atom has an electronic structure similar to that of the carbon atom, and all five of its own valence electrons can combine with the carbon atom, thus inducing an upward shift in the Fermi energy level and conduction band electrons, which in thus improve the optical properties of CQDs.[111] More interestingly, nitrogen atoms can also enhance quantum yields by modulating defect vacancies on the surface of CQDs.[39,112] When the reaction precursor contains only –OH or –COOH, the quantum yield is often below 10%, but when an amino group is introduced into it, the quantum yield can reach 80%.[106] Therefore, when selecting precursors, we can enhance the quantum yield of CQDs by directly using biomass materials containing nitrogen or by adding some organic small molecules containing heteroatoms.

CQDs with 99% quantum yield can be synthesized by microwave heating using ethanolamine, citric acid and tris(hydroxymethyl)aminomethane as reactants, mainly because during the heating process, the amino and carboxyl groups of the carbon source will form amide bonds through dehydration condensation, modifying the hydroxyl structure on the surface of CQDs.[113] CQDs with a quantum yield of 94.5% could be prepared by hydrothermal method using folic acid with a high nitrogen content as precursor. Here, in addition to the role played by the dehydration condensation of amino and carboxyl groups, the PH environment also plays a very important role in the fluorescence intensity and quantum yield of CQDs.[114]

CQDs with a quantum yield of 94% and bright blue fluorescence can be synthesized by hydrothermal methods using citric acid and ethylenediamine as reaction precursors. In this reaction, hydrothermal conditions induce dehydration condensation of the amino group with the carboxyl group to form an amide bond, which then dehydrogenates with the neighbouring carboxyl group to form pyrrole N, which is converted to graphite N under hydrothermal conditions. Therefore, N doping greatly improved the quantum yield and fluorescence properties of CQDs.[115] Some studies have also shown that pyridine N and pyrrole N can induce a blue shift in the fluorescence of CQDs and increase the quantum yield of CQDs.[107,116]

In addition to nitrogen, sulfur, boron and phosphorus are also commonly used in CQDs doping. Do[117] et al. prepared S-CQDs using 2,2′-(ethylenedithio)diacetic acid and applied it to light-emitting diodes. The test shows that the electronic states induced by direct doping have a very important influence on the luminescent properties of CQDs. Shan[118] et al. successfully prepared a high-fluorescence B-CQDs by reacting hydroquinone with boron tribromide by solvothermal method. This is due to the electron transfer between doped boron atoms and hydrogen peroxide, which induces hydrogen peroxide to produce an effective fluorescence quenching effect. At present, B-CQDs has been successfully applied in the fluorescence analysis system of glucose and hydrogen

peroxide. Zhou[119] et al. successfully prepared a P-CQDs with adjustable emission wavelength and high fluorescence emission efficiency by solvothermal method using phosphorus tribromide and hydroquinone.

Co-doping

The interaction of many elements can produce many unique electronic structures, which has successfully stimulated the interest of researchers. Ye[120] et al. successfully prepared four kinds of high-fluorescence S–N-CQDs using pigeon eggshell, feathers, egg yolk and feces as carbon precursors, and their corresponding quantum yields were 17.48%, 24.87%, 16.34% and 33.50%, respectively. Tan[121] et al. used 1,2-hexadecanediol, melamine and sodium borate as reaction raw materials to synthesize N–B-CQDs with good optical properties through pyrolysis, which has great potential in optics and sensing. In addition, some researchers have successfully prepared N–F-CQDs.[122]

Although there have been some relevant studies on doped CQDs at present, the research scope of this project is relatively narrow. For example, the types of doped elements are very few, and the mechanism of luminescence properties also needs to be studied. In addition, most researchers use organic small molecules or polymers to directly synthesize CQDs, while few use biomass raw materials to directly synthesize doped CQDs. Therefore, in the future research, on the one hand, we can select natural biomass rich in N, S, P and other elements as the reaction raw material, which not only makes the process of preparing CQDs relatively simple, but also provides non-metallic atoms, which can effectively improve the quantum yield and optical properties. On the other hand, we can choose biomass containing certain elements as raw materials and then add heteroatomic dopants as needed. This method can not only reduce the difficulty of carbon source selection, but also achieve the co-doping of multiple elements.

Size distribution modulation of CQDs

The particle size of CQDs is usually within the range of 0–10 nm, and the different size distribution may be one of the main factors for the formation of tunable photoluminescence of CQDs. Therefore, the fluorescence properties of CQDs can be regulated by changing their nano-size distribution.

Sk[107] et al. have theoretically analyzed and calculated the fluorescence mechanism of graphene CQDs by using density functional theory and time-dependent density functional calculations. As shown in Fig. 14, with the increasing particle size, the fluorescence emission of graphene CQDs is also continuously redshifted. Some scientific researchers have successfully prepared CQDs with blue, green, and yellow fluorescence emission by taking Manilkara zapota[30] and Mango[31] as reaction carbon sources, using sulfuric acid and phosphoric acid reagents, and controlling their reaction temperature in different ways. By observing the particle size, it can be seen that the particle size is increasing and the fluorescence color is gradually changing from blue to yellow. Similarly, Diao et al.[32]
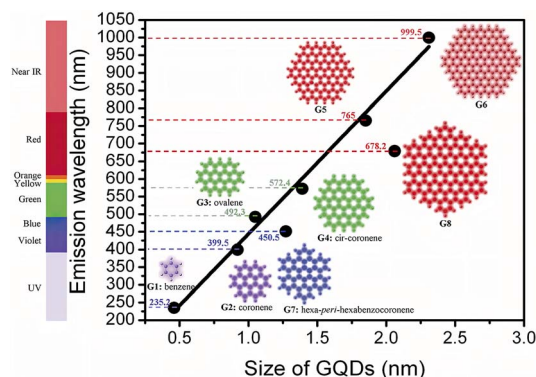
Fig. 14 Relationship between particle size and luminescence wavelength of graphene CQDs.[107] "Reproduced from ref. 107 with permission from [Royal Society of Chemistry], copyright [2023]".

used *Syringa oblata* Lindl. as the precursor and finally successfully prepared CQDs with blue and green fluorescence by changing the solution of the reaction process. In the process of probing the particle size, scholars found that the fluorescence emission redshift of CQDs is related to its size increase.

Therefore, the size distribution of CQDs is one of the important factors affecting its fluorescence emission. In the future, we can change the fluorescence emission color of CQDs by changing the conditions of the preparation process and adjusting the size distribution of CQDs.

Application of biomass CQDs

Compared with inorganic semiconductor CQDs and fluorescent materials, biomass CQDs have good fluorescence stability, biocompatibility, low toxicity and strong water solubility, and are easy to prepare and surface modify.[123] And replacing the reaction precursor with renewable natural raw materials can greatly reduce the preparation cost of CQDs and improve the yield. These advantages make biomass CQDs a promising green material. At present, this material is currently used in many fields such as ion detection, bio-imaging, biomedicine, biosensing, solar cells, catalysis, optoelectronic materials, anticounterfeiting materials and many others.

Ion detection

Specific structures or groups on the surface of biomass CQDs can exhibit fluorescence quenching effects on some metal ions.[124,125] Both electron transfer and its internal filtering effect will lead to fluorescence quenching effect.[126,127] By using two CQDs fluorescence modes (turn-off or turn-off-on) to construct fluorescent probes, the detection of specific ions can be realized. In addition, this method can effectively solve the problems of cumbersome process and high cost of traditional detection methods.

Detection of Fe^{3+}, Hg^{2+} and Cu^{2+} ions

In recent years, heavy metal pollution has seriously threatened human health and ecological security. Excessive intake

of iron, mercury, copper and other metal elements with very similar chemical properties[128] will cause great harm to human body. For example, excessive Fe^{3+} exists in the human body, which will lead to cancer, diabetes and other diseases;[129,130] long-term intake of Hg^{2+} will cause nephritis, proteinuria and other diseases;[131,132] excessive intake of Cu^{2+} will seriously damage human liver function and kidney function. Therefore, the detection of iron, mercury, copper and other heavy metal ions is very important for human beings and the ecological environment. The traditional nanomaterials used for the detection of Fe^{3+}, Hg^{2+}, Cu^{2+} and other metal ions mainly include metal nanoclusters,[133] organic molecular fluorescence probes,[134] semiconductor quantum dots,[135] rare earth complex materials,[136] rare earth doped fluorescent nanoparticles[137] and fluorescent probes based on ordered mesoporous materials.[138] Although these materials can generally achieve the detection of most heavy metal ions, they generally have problems such as low detection limits, cumbersome synthesis processes, long detection times, and high costs. In addition, the raw materials used in the synthesis of these materials are mostly organic reagents and metal ions with some toxicity. Even if the content is low, it will produce high biological toxicity, which limits its application in multiple fields such as food and biological testing. However, if biomass-based synthesis of CQDs is applied to ion detection, then the use of natural non-toxic precursor is not only greener at the source, the synthesis process is easier, and the detection time and cost will be reduced compared to the previous. Most importantly, compared with traditional nanomaterials, biomass CQDs have higher sensitivity, better light stability, structural stability and excellent adjustability, so they will have greater advantages in ion detection.

At present, several common metals detected by biomass CQDs include Fe^{3+}, Hg^{2+} and Cu^{2+}. These metals can cause fluorescence quenching of biomass CQDs. Therefore, we can test the existence of these ions through their fluorescence quenching phenomenon.[169]

As shown in Tables 3–5, at present, these biomass materials have been successfully used for the detection of Fe^{3+}, Hg^{2+} and Cu^{2+}. Traditional detection methods, such as atomic absorption spectrometry, electrochemical detection, atomic fluorescence spectrometry, *etc.*,[139] have low detection limit, wide detection range, high cost, complicated process and large error. Compared with the traditional detection methods, the synthesis process, operation process, detection range, and minimum detection limit of biomass CQDs have shown certain advantages.

Other ion detection

In addition to the above three metal ions Fe^{3+}, Hg^{2+} and Cu^{2+}, biomass CQDs can also detect other metal ions through other phenomena or mechanisms. In some related literature, we found that researchers have used biomass CQDs to detect Pb^{2+},[86,160] V^{5+},[161] Al^{3+},[162] Co^{2+},[163] Cr^{6+} (ref. 164 and 165) Ag^+ (ref. 25) and other metal ions. Among them, Sahu *et al.*[21] used Saint Basil as carbon source to prepare CQDs by hydrothermal

Table 3 Fe^{3+} ion detection

Biomass carbon source	Synthesis method	Range of tests	Detection limit	Ref.
Rose heart radish	Hydrothermal method	0.02–40 μM	0.13 μM	140
Magnolia	Hydrothermal method	0.2–100 μM	0.073 μM	87
Jinhua perfumed lemon	Hydrothermal method	0.025–100 μM	0.075 μM	141
Astragalus herb	Hydrothermal method	50–250 μM	42 nM	142
West Indian gooseberry	Hydrothermal method	2–25 μM	0.9 μM	143
Reishi spores	Hydrothermal method	2.5–100 nM	15.9 nM	144
Bauhinia	Microwave method	40–350 μM	0.01 μM	95
Sweet potato	Hydrothermal method	1–100 μM	0.32 μM	145
Pine wood	Hydrothermal method	0–2000 μM	355.4 nM	146
Gelatine	Hydrothermal method	0–50 μM	0.2 μM	147

Table 4 Hg^{2+} ion detection

Biomass carbon source	Synthesis method	Range of tests	Detection limit	Ref.
Jinhua perfumed lemon	Hydrothermal method	0.01–100 μM	5.5 nM	141
Mushrooms	Hydrothermal method	0–100 nM	4.13 nM	148
Lilies leaves	Pyrolytic carbonisation	5–500 ng mL^{-1}	6.3 nM	149
Citrus lemon	Hydrothermal method	0.001–1 μM	5.3 nM	132
Pigeon feather	Pyrolytic carbonisation	0–1.2 μM	10.3 nM	120
Eggshell film	Hydrothermal method	10–100 μM	2.6 μM	150
Citric acid	Hydrothermal method	0.1–1.2 μM	20 nM	151

Table 5 Cu^{2+} ion detection

Biomass carbon source	Synthesis method	Range of tests	Detection limit	Ref.
Carrot	Hydrothermal method	1–5 μM	6.8 μM	152
Acacia seeds	Microwave method	0.01–10 μM	4.3 nM	153
Bran	Solvent heat method	0–0.5 mM	0.0507 μM	154
Bananas	Hydrothermal method	100–800 μg mL^{-1}	0.3 μg mL^{-1}	155
Eleusine coracana	Pyrolytic carbonisation	0–100 μM	10 nM	156
Grape seeds	Hydrothermal method	150–500 μg mL^{-1}	0.048 mg L^{-1}	157
Petals	Pyrolytic carbonisation	0–190 μM	200 nM	158
Coffee grounds	Hydrothermal method	0–1 μM	—	159

method, which can be used for selective test of Pb^{2+}. This selectivity is mainly due to the high binding affinity between the empty d orbital of Pb^{2+} ion and the surface amine group of CQDs. The amine-based nitrogen atoms on the surface of CQDs transfer electrons to the empty d orbital of Pb^{2+} ion and generate non-radiative electron transfer, which makes CQDs and Pb^{2+} ions better complexed, so that Pb^{2+} ions can effectively quench the fluorescence of CQDs. Its detection range is 0.01–1.0 μM. LOD is 0.59 nmol L^{-1}. Shuang et al.[163] adopt pig skin as carbon source to prepare N-CQDs to detect Co^{2+}. The fluorescence emission spectrum of N-CQDs overlaps with the Co^{2+} absorption band, so the fluorescence of N-CQDs can be significantly quenched through the Co^{2+} internal filtering effect. The detection range of the N-CQDs is 1.0×10^3–3.0×10^5 nmol L^{-1}, and the LOD is 680 nmol L^{-1}.

Currently, some researchers have also carried out studies on the fluorescence mechanism of Cr^{6+}, including reduction reaction[166] and coordination between groups and Cr^{6+}.[167] In addition, Cr^{6+} has a d orbital and low d–d transition state, which can greatly promote the non-radiative recombination of holes and electron pairs, thus leading to the fluorescence quenching of biomass CQDs.[168]

Bioimaging

Semiconductor quantum dots, organic dyes, luminescent nanomaterials and various luminescent substances have been widely used in biological imaging. However, these materials have low fluorescence brightness, poor photostability and low solubility, and contain heavy metal ions and organic reagents with high biological toxicity. This severely limits its application in medicine, fluorescent labeling and other fields, and also brings irreversible harm to human beings and ecological environment. On the contrary, the emerging biomass CQDs prepared by using green raw materials have lower biological toxicity and side effects. In addition, CQDs synthesized from biomass have the advantages of stable fluorescence emission, matt bleaching, biocompatibility and good cell membrane

penetration, so it is expected to replace traditional materials and be better applied in the biological field.

In recent years, the application of CQDs in the field of biological imaging mainly includes the detection of animal cells, plant cells and microorganisms,[28,171] which can help people better understand the mechanisms and various biological processes in cells. For example, the fluorescence effect of CQDs can be used to locate different regions inside cells (mainly including nucleus, cell membrane and cytoplasm),[106] observe cell phenotypes and monitor intracellular processes in real time,[172] *etc.*

Sun's[18] research group reported for the first time the application of CQDs in the field of biological imaging. They observed *E. coli* CC25922 cells labeled with CQDs and CQDs entering Caco-2 cells using confocal microscopy. As shown in Fig. 15, we can find that they show bright fluorescence and exhibit many excellent properties. This discovery attracted many researchers to do research in this field, and several years later, biomass CQDs were widely used in the field of biological imaging. Miao *et al.*[83] successfully prepared CQDs with turn-off-on fluorescence emission mode using tomato as raw material to realize fluorescence imaging of carcinoembryonic antigen. This is mainly because under π–π interaction, a large number of
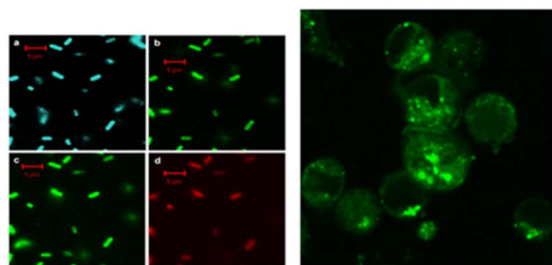

Fig. 15 Fluorescence imaging of CQDs-labelled *E. coli* ATCC25922 cells (left) and CQDs entering Caco-2 cells (right).[18] "Reproduced from ref. 18 with permission from [American Chemical Society], copyright [2023]".
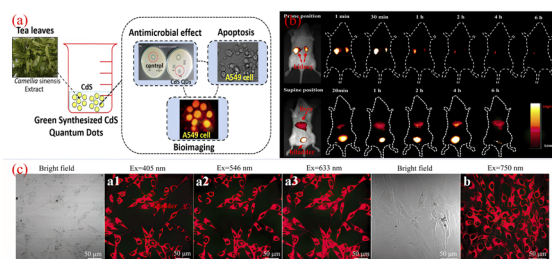

Fig. 16 (a) Schematic diagram of CQDs prepared from tea leaves as raw material and used for *in vitro* imaging of A549 cancer cells.[173] (b) Time-dependent imaging map of CQDs injected *via* tail vein in mice.[175] (c) Single-molecule mode (a1–a3) and bimolecular mode (b) fluorescence imaging maps of CQDs.[174] "Reproduced from ref. 173 with permission from [American Chemical Society], copyright [2023]". "Reproduced from ref. 175 with permission from [American Chemical Society], copyright [2023]". "Reproduced from ref. 174 with permission from [John Wiley and Sons], copyright [2023]".

carboxyl groups in CQDs are attracted to ssDNA and produce ssDN-CQDs, which leads to fluorescence quenching. Since the binding force between ssDNA and carcinoembryonic antigen is greater than that between ssDNA and CQDs, we can restore the fluorescence properties of CQDs by applying carcinoembryonic antigen, and the detection accuracy of this method is relatively accurate, with a detection limit as high as 0.3 ng mL^{-1}. As shown in Fig. 16(a), Shivaji *et al.*[173] synthesized CdS-CQDs using tea extract as precursor, which can be used for *in vitro* imaging of A549 cancer cells. By flow cytometry analysis, the researchers found that CQDs had good reactivity and stability, and could well inhibit the further growth of A549 cancer cells. Liu *et al.*[174] synthesized CQDs with deep red fluorescence using *Taxus chinensis*, which showed strong fluorescence emission performance and good biocompatibility in the dark red region, so it was often used as a fluorescence probe for monomolecular and bimolecular biological imaging. By observing Fig. 16(c), we can find that bright dark red fluorescence can be observed in both single molecular mode Fig. 16(a1)–(a3) and bimolecular mode Fig. 16(b1). Li *et al.*[175] synthesized a new type of CQDs material with the second near-infrared emission using watermelon as the carbon source. The CQDs prepared by this method have low toxicity, high QY yield and good biocompatibility. As shown in Fig. 16(b), these CQDs can be injected into the mouse body to image the mouse body through near-infrared emission. Interestingly, through fluorescence imaging, it can be seen that the excretion rate of CQDs in mice is related to their particle size. Jeong *et al.*[31] synthesised yellow, green and blue CQDs using mangoes under different acidification conditions, and injected the CQDs into the tails of nude mice. 24 h later, blue and green CQDs were present in the bladder, while yellow CQDs remained inside the liver, suggesting that blue and green CQDs were cleared more rapidly, while yellow ones were cleared more slowly. In addition, some scholars believe that CQDs may accelerate transmission through urine after relevant studies.[58]

In addition, the particle size of biomass CQDs also has a very important effect on cell imaging. Chen *et al.*[176] mixed sucrose with oleic acid, and then obtained CQDs by hydrothermal method. This CQDs have been used to label human bronchial epithelial cells. Researchers have also found that CQDs can easily enter the cell membrane and cytoplasm, but it is difficult to enter the nucleus. Shi *et al.*[177] prepared a CQDs with an average diameter of 2.49 ± 0.13 nm and good cell penetration using a variety of different plant petals as initial carbon sources. This CQDs have been used in cell imaging of human cervical squamous cell carcinoma, and can penetrate cell membranes well and be localized into the nucleus.

Biomedicine

At present, the efficient targeted drug delivery technology is not perfect enough. For example, when some anticancer drugs and chemotherapy drugs are imported into the human body, their diffusion and distribution direction cannot be accurately estimated, so that they are widely distributed in the human body, causing irreversible harm to healthy cells and tiny tissues in the body while eliminating viral cells. Therefore, how to efficiently

and minimize the harm of drugs to human body has become the focus of current researchers. In recent years, biomass CQDs, with its excellent properties, has been shining brightly in a variety of applications. It has also had a remarkable effect on drug delivery and construction. By using the property that the surface of biomass CQDs is easy to be doped and modified, it can well realize the complexation with different drugs, thus completing the delivery of various drugs. In addition, biomass CQDs play a very important role in clinical disease diagnosis, treatment and real-time tracer due to their excellent optical properties, low toxicity and other advantages.[29,178]

N. Mehta et al.[179] synthesized CQDs by one-step hydrothermal method using pasteurized milk as raw material. After coupling the CQDs with Lisinopril, a novel drug carrier was formed, which was conducive to effectively delivering Lisinopril to HeLa cells and monitoring cell uptake into the drug delivery system at the same time. At the same time, the adoption of this vector can have a very significant HeLa cell survival rate, which plays a very important role in the targeted treatment of cancer and hypertension. Chang et al.[180] mixed crab shells with three kinds of transition metal ions respectively, and obtained CQDs doped with three kinds of metal ions by microwave method. Using folic acid targeting group (FA) and gadolinium doped CQDs, we prepared a CQDS-FA fluorescent probe that acts as a targeted fluorescent sensor for cancer cells and can also be used to deliver adriamycin. In the HeLa cell experiment, it was found that adriamycin delivered by CQDs has a stronger pharmacodynamic effect than adriamycin alone, so CQDs can also be proved to be a delivery platform with enhanced drug effect. D'souza et al.[181] synthesized CQDs from shrimp by one-step hydrothermal method, and successfully constructed a traceable drug delivery platform for targeted delivery to MCF-7 cells. This is mainly because Berdine interacts with the surface of CQDs through non-covalent interaction to complex them together.
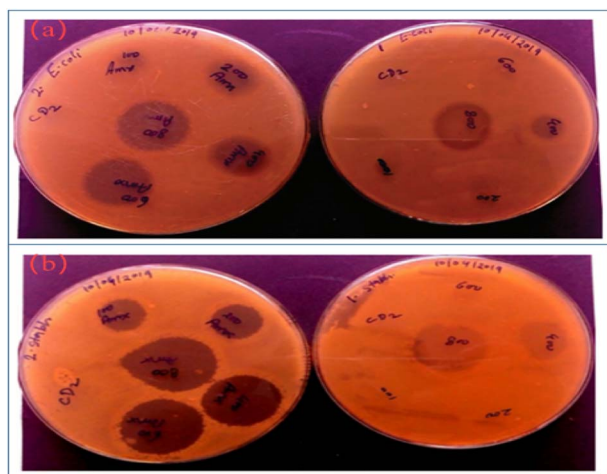
When the complex enters the tumor cells, MCF-7 cells gradually release choline from the loaded CQDs through endocytosis, which greatly enhances the concentration of the drug and thus plays a role in enhancing the cytotoxicity of the drug. As the cells can take up fluorescence, so it can not only be used as a tumor therapeutic agent, but also an ideal fluorescent probe for tracking cancer cells.

In addition to being used to treat and track cancer cells, CQDs also play a vital role in bacterial infection treatment and bacterial tracking detection. Ahmadian-Fard-Fini et al.[182] prepared CQDs from lemon and grapefruit extracts, and complexed them with Fe_3O_4 particles to successfully prepare a non-toxic and sensitive fluorescent probe for detecting *Escherichia coli*. Through the experiment, the researcher concluded that between 0–9 × within 107 cfu mL^{-1}, the increasing number of *Escherichia coli* will cause fluorescence quenching of CQDs. John et al.[183] used wheat bran as the initial carbon source to synthesize CQDs with a quantum yield (QY) of up to 33.23%, and then compounded amoxicillin (AMX) onto the surface of CQDs to develop a new drug delivery system that could be used for AMX. It can be seen from Fig. 17 that CQDs-AMX has very obvious inhibitory effect on *Escherichia coli* and *Staphylococcus aureus*, and its toxicity is small.

Biosensing

Biomass CQDs has excellent and unique optical properties, which makes it have a very wide range of applications in biosensing, biomedicine and other aspects. It is worth noting that the abundant functional group structure on the surface can make the interaction between biomolecules, so that the fluorescence intensity of biomass CQDs has a significant change.

Fig. 17 (a) Left: *E. coli* treated with CQDs and amoxicillin, right: *E. coli* treated with CQDs–AMX complex; (b) *Staphylococcus aureus* treated with CQDs and amoxicillin, right: *Staphylococcus aureus* treated with CQDs–AMX complex.[183] "Reproduced from ref. 183 with permission from [John Wiley and Sons], copyright [2023]".
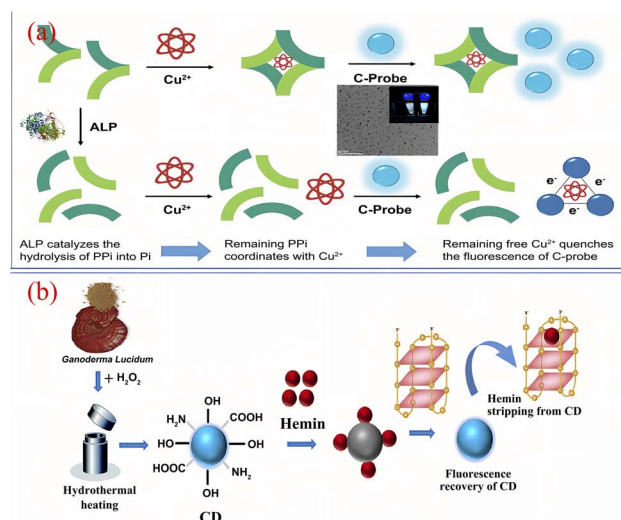

Fig. 18 (a) Schematic diagram of Cu^{2+} assisted biomass CQDs for alkaline phosphatase detection[184] (b) schematic diagram of efficient detection of G-quadruplex based on biomass CQDs.[188] "Reproduced from ref. 184 with permission from [Elsevier], copyright [2023]". "Reproduced from ref. 188 with permission from [Elsevier], copyright [2023]".

During this period, some substances can complexate with biomass CQDs to induce fluorescence quenching, while others can significantly enhance the fluorescence of biomass CQDs. Therefore, we can judge whether the purpose of specific detection is achieved through these two phenomena.

At present, researchers have successfully applied biomass CQDs to the specific detection of biomolecules. Kim[184] et al. successfully synthesized a biomass CQDs with bright blue fluorescence using vegetable waste under ultrasonic treatment, and then they successfully constructed a highly sensitive and real-time fluorescence assay method for monitoring alkaline phosphatase activity. As shown in Fig. 18(a), this method mainly uses Cu^{2+} to induce fluorescence quenching of biomass CQDs, and alkaline phosphatase can inhibit the selective coordination between pyrophosphoric acid and Cu^{2+}. After pyrophosphate is added, it can be found that the preferential complexation of Cu^{2+} with it is far greater than that of Cu^{2+} with biomass CQDs. When alkaline phosphatase is present, pyrophosphate undergoes a hydrolysis reaction and is converted into phosphate, thereby inhibiting its interaction with Cu^{2+} and leading to significant fluorescence quenching. After testing and analyzing the actual samples, the dynamic detection linear range is 0.5–10 nM. Therefore, this biomass CQDs can be applied for precise detection of alkaline phosphatase activity.

Biomass CQDs can not only be used for protein specific detection, but also for DNA specific detection.[185] Pramanik[186] et al. synthesized a biomass CQDs with blue fluorescence using eggshell membrane as a carbon source. After extensive research, it was found that the fluorescence effect of the biomass CQDs was enhanced after complexing with the DNA corresponding to the adenine thymine (AT) base pair, while there was no phenomenon after complexing with the DNA corresponding to the guanine cytosine (GC) base pair. Therefore, we can see that the biomass CQDs have excellent selectivity and strong affinity for DNA corresponding to AT bases. Godavarthi[187] et al. used sargassum as raw material to synthesize a CQDs fluorescence sensing system capable of efficiently detecting DNA. When single stranded DNA, double stranded DNA, and RNA are used to label the biomass CQDs, the fluorescence intensity of the system can be significantly enhanced. Therefore, the biomass CQDs can be used as green non-toxic fluorophores to realize the visual detection of nucleic acid. Kumari[188] et al. used Ganoderma lucidum as a precursor to prepare nitrogen-doped high-fluorescence biomass CQDs by one-step hydrothermal method, and successfully applied it to the efficient fluorescence detection of G-quadruplex. As shown in Fig. 18(b), the biomass CQDs is conjugated with heme chloride, resulting in the fluorescence quenching of biomass CQDs. With the slow addition of G-quadruplex in DNA, G-quadruplex will be complexed with heme chloride in priority, so that the bonded heme chloride on the surface of biomass CQDs will gradually fall off, and its fluorescence will gradually recover. After fluorescence recovery, fluorescence emission can be observed by simple ultraviolet irradiation. Therefore, we can use this to test the G-tetrad. The drawback is that this method can only be applied to G-quadruplex containing DNA, and cannot be used for other DNA sample detection. Therefore, how to better use biomass CQDs to detect DNA sequence specificity is still a big challenge for us today.

Solar cell

CQDs not only have special optical properties, but also have a wide range of light absorption capabilities and upconversion advantages. In recent years, researchers have successfully applied CQDs to the field of solar cells based on these characteristics.[189,190] Scholars have found that the efficiency of batteries can be effectively improved by promoting the separation of photogenerated electron–hole pairs, inhibiting the recombination of carriers, improving the absorption range, and promoting carrier separation and electron extraction. At present, CQDs is mainly applied in solar cells in three forms: light absorber, transport layer and photosensitizer.[191] However, most of the materials related to CQDs used in the production of solar cells are very expensive, such as some organic reagents, rare metal materials, etc., which will bring unaffordable economic pressure to enterprises and scientific research institutions. Therefore, in recent years, in order to reduce the cost of solar cells and synthetic photosensitizers, researchers have adopted green, environmentally friendly and easily accessible biomass-based materials to prepare biomass CQDs. The following section will mainly introduce the latest research progress in the application of biomass CQDs in solar cells in recent years.

Wang[192] et al. synthesized a kind of biomass CQDs with ultra-high fluorescence properties by one-step hydrothermal method using completely green Ginkgo biloba leaves and auxiliary materials. By combining the CQDs with EVA, scholars successfully developed a CQDs/EVA thin film with high photoelectric conversion efficiency (PCE). After coating 0.050% CQDs/EVA thin film on the surface of polycrystalline silicon solar cells, the photovoltaic conversion efficiency of solar cells increased from 13.19% to 13.65%. This discovery greatly improves its application effect in photovoltaic, environment, energy and other fields. Marinovic[193] et al. prepared various types of biomass CQDs using various biomass materials. By comparing these biomass CQDs, scholars carefully analyzed the chemical structure, physicochemical properties, and photoelectric properties of each type of CQDs, and successfully applied them to the photosensitizer of TiO_2 nanostructured solar cells. Among them, the photoconversion efficiency of L-arginine carbon nanodots was the highest (0.36%), and that of lobster shell carbon nanodots was 0.22%. Interestingly, the researchers also found that functionalizing carboxylic acids with amines is a very good way to improve the performance of solar cells. Meng[194] et al. took soybean powder as raw material, prepared CQDs by one-step hydrothermal method, combined it with TiO_2 anode, and successfully built a new all-weather biomass CQDs solar cell. This battery can not only capture more solar energy and store a large amount of light, but also generate electricity in both day and dark, providing a maximum dark light to electricity conversion efficiency of 7.97%. Similarly, Liu[195] et al. successfully prepared biomass CQDs with high fluorescence performance by taking lotus as raw material and supplementing sulfur or nitrogen atoms in it. When applying this CQDs to the
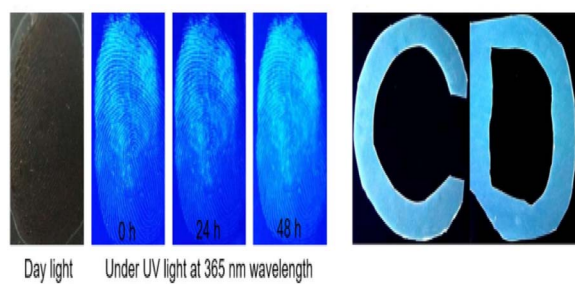
Fig. 19 Application of CQDs prepared from shiitake mushrooms for fingerprint detection and CQDs/PMMA composites.[196] "Reproduced from ref. 196 with permission from [Elsevier], copyright [2023]".

light absorber of mesoscopic solar cells, the light collection efficiency and electron extraction ability were greatly improved, resulting in maximum light conversion efficiency of 0.158% and 0.208% in two-stage and tertiary photovoltaics, respectively. Subsequently, in order to further enhance the ability to extract electrons, researchers integrated CQDs with N719 dye and successfully prepared a photosensitive device with a light conversion efficiency of up to 9.04%. Therefore, from these research findings, we can see that biomass CQDs have enormous potential value in preparing high optical performance solar cell.

Development of potential applications for biomass CQDs

Biomass CQDs have very good fluorescence properties and biocompatibility, so they are widely used in ion detection, biological imaging, biomedicine. In addition, biomass CQDs also has excellent physical and chemical properties, photoinduced electron transfer ability, excitation light dependence, *etc.*, which can make it widely used in capacitor, anti-counterfeiting materials, photocatalysis and other fields in the future.[23,197]

Hoang *et al.*[88] used cauliflower leaves as precursor to synthesize N-CQDs by one-step hydrothermal method, and then synthesized them with reduced GO through hydrothermal reaction to successfully prepare a CQDs/reduced GO electrode material with high specific capacitance. Among them, doped nitrogen has a significant impact on the active sites of CQDs. In addition, CQDs effectively block the re-stacking of graphene, and make its surface area and pore volume larger, thus changing the electrochemical characteristics of RGO. Another scholar[196] used *Lentinus edodes* as natural carbon source precursor and obtained CQDs with bright blue fluorescence by hydrothermal method. As shown in Fig. 19, when it is applied in the field of fluorescent composite materials and fingerprint imaging, it still presents clear fingerprint imaging after a long time of laser irradiation test, showing that this CQDs has excellent optical stability. The researchers then combined the CQDs with PMMA to form a CQDs/PMMA material with better fluorescence properties. This material can show a unique bright blue fluorescence under ultraviolet light, so it can be used in anti-counterfeiting technology. Prasannan *et al.*[84] prepared CQDs containing a large number of oxygen functional groups by one-step

hydrothermal reaction using orange peel as the reaction material, and then synthesized them with ZnO to successfully prepare a ZnO/CQDs composite material, which was successfully applied in the photocatalyst of blue naphthol azo dyes. In addition, the CQDs also has a large specific surface area and excellent electron transfer performance, which makes the degradation rate and degree of the composite far exceed the degradation effect of ZnO alone.

Although the current research on biomass CQDs is still in the initial stage, it has shown profound development potential in ion detection, biological imaging, biomedicine, photocatalysis, anti-counterfeiting materials, capacitors and other fields, which will provide great help for clinical medicine, scientific research and other fields in the future.

Conclusion

This article mainly provides a detailed analysis of the optical properties, fluorescence mechanism, synthesis methods, fluorescence regulation, and other aspects of biomass CQDs, revealing the optical properties, main mechanism of fluorescence emission, and synthesis methods of biomass CQDs. In addition, this paper also introduces the reasons why biomass CQDs produce different fluorescence spectra and how to effectively regulate their fluorescence performance, which provides a basis for the preparation of biomass CQDs with high quantum yield and multiple fluorescence colors. Through comprehensive analysis, it is not difficult to conclude that the preparation process of biomass CQDs and its surface functional group structure, heteroatoms and particle size distribution all have important effects on fluorescence intensity, quantum yield and fluorescence emission wavelength. Finally, this article provides a comprehensive analysis and problem summary of the research progress of biomass CQDs in the fields of ion detection, biological imaging, biomedicine, biosensing, solar cells, anti-counterfeiting materials, photocatalysis, and capacitors in recent years.

Challenges and future prospects

In 2004, a new type of carbon based nanomaterials (CQDs) emerged. With its unique optical properties, photostability, biocompatibility, water solubility, low cost, and other advantages, this material has been widely used in various fields such as biological imaging, sensing, optoelectronic devices, catalysis, *etc.* However, in the preparation process, researchers mostly use organic small molecules or metal materials as raw materials or auxiliary reagents, which will result in the produced CQDs having partial biological toxicity and irreversible harm to humans and the ecological environment. Therefore, how to prepare green, environmentally friendly, and non-toxic CQDs has become an extremely important scientific issue at present. Biomass materials are not only environmentally friendly and have low toxicity, but also have a lot of heteroatoms and functional groups. Therefore, they are not only expected to become the best material for preparing biomass CQDs, but also can greatly

reduce the negative effects brought by traditional materials. Biomass CQDs have been gradually developed after many years. Compared with traditional CQDs, CQDs prepared using biomass as raw materials not only has better fluorescence performance, optical stability and coordinated emission wavelength ratio, but also has simple synthesis process, low raw material cost and low biological toxicity, which greatly improves the feasibility of green process and environmental protection. However, in the aspect of specific application, it still has certain limitations and undeveloped, the following are our summary of the specific problems and its future prospects.

We believe that the current problems and expandable directions of biomass CQDs mainly include: (1) for the problem of single fluorescence color of biomass CQDs, we can start from the prepared multi fluorescence emitting biomass CQDs materials, and comprehensively summarize and summarize their reaction conditions, surface functional groups, surface functionalization modifications, and particle size regulation. On this basis, continue to conduct experiments and verify, and then obtain the best method and conditions for precise regulation of fluorescence color. (2) The fluorescence emission of CQDs is mainly based on its own unique structure and functional groups. Only by constantly studying the structure can we better understand its fluorescence mechanism. Therefore, it is very important to develop new characterization methods for biomass CQDs structure detection. (3) Biomass CQDs is only suitable for simple laboratory production and cannot be large-scale production due to its difficult separation and purification. Therefore, the development of a new simple and environmentally friendly separation and purification means will become the main development direction to achieve large-scale production. (4) Biomass CQDs has been successfully used in biomedicine-related fields on a large scale by virtue of its advantages of environmental protection and low toxicity. However, in addition, biomass CQDs also possess many potential properties such as photoinduced electron transfer ability and catalytic ability, which have not been fully developed and utilized at present. Therefore, it is extremely important to actively explore the potential properties of biomass CQDs and develop their related applications in other fields. We believe that in the near future, we can explore other application value of birth substance CQDs, and widely apply it to practical engineering applications, to provide more convenience for the society and even the whole world.

Author contributions

Lei Wang: manuscript writing, data processing, article layout; Shujia Weng: photo design, data collection; Shuai Su: data collection and collation; Weiwei Wang: thesis ideas, logical content design.

Conflicts of interest

There are no conflicts to declare.

Notes and references

1 C. V. Raju, C. H. Cho and G. M. Rani, *Coord. Chem. Rev.*, 2023, **476**, 214920.
2 Y. Zhao, R. Nakamura and K. Kamiya, *Nat. Commun.*, 2013, **4**(1), 2390.
3 M. Barberio and P. Antici, *Sci. Rep.*, 2017, **7**(1), 12009.
4 B. S. Miller, L. Bezinge and H. D. Gliddon, *Nature*, 2020, **587**(7835), 588–593.
5 S. Zhang, S. Jiang and B. Huang, *Nat. Sustain.*, 2020, **3**(9), 753–760.
6 J. Yuan, T. Huang, P. Cheng, Y. Zou and H. Zhang, *Nat. Commun.*, 2019, **10**(1), 570.
7 X. He, H. Htoon, S. K. Doorn, W. H. P. Pernice and F. Pyatkov, *Nat. Mater.*, 2018, **17**(8), 663–670.
8 M. Sirignano, C. Russo and A. Ciajolo, *Carbon*, 2020, **156**, 370–377.
9 X. Zhou, Z. Tian, J. Li, H. Ruan, Y. Ma, Z. Yang and Y. Qu, *Nanoscale*, 2014, **6**(5), 2603–2607.
10 X. Wang, A. Dong, Y. Hu, J. Qian and S. Huang, *Chem. Commun.*, 2020, **56**(74), 10809–10823.
11 S. Xu, A. Dong, Y. Hu, Z. Yang, S. Huang and J. Qian, *J. Mater. Chem. A*, 2023, **11**, 9721–9747.
12 Y. Liang, Y. Shen, C. Liu and X. Ren, *J. Lumin.*, 2018, **197**, 285–290.
13 S. Yang, X. Wang, P. He, A. Xu and G. Wang, *Small*, 2021, **17**(10), 2004867.
14 A. Rezaei, L. Hadian-Dehkordi, H. Samadian, M. Jaymand and H. Targhan, *Sci. Rep.*, 2021, **11**(1), 4411.
15 K. Hola, Y. Zhang and Y. Wang, *Nano Today*, 2014, **9**(5), 590–603.
16 S. Zhu, Y. Song, X. Zhao, J. Shao, J. Zhang and B. Yang, *Nano Res.*, 2015, **8**, 355–381.
17 X. Xu, R. Ray, Y. Gu, H. J. Ploehn and L. Gearheart, *J. Am. Chem. Soc.*, 2004, **126**(40), 12736–12737.
18 Y. Sun, B. Zhou, Y. Lin, W. Wang, K. A. S. Fernando and P. Pathak, *J. Am. Chem. Soc.*, 2006, **128**(24), 7756–7757.
19 Y. Zhang, Z. Gao, W. Zhang, W. Wang, J. Chang and J. Kai, *Sens. Actuators B Chem.*, 2018, **262**, 928–937.
20 V. Roshni, S. Misra, M. K. Santra and D. Ottoor, *J. Photochem. Photobiol. A*, 2019, **373**, 28–36.
21 A. Kumar, A. R. Chowdhuri, D. Laha, T. K. Mahto, P. Karmakar and S. K. Sahu, *Sens. Actuators B Chem.*, 2017, **242**, 679–686.
22 H. Liu, L. Ding, L. Chen, Y. Chen, T. Zhou, H. Li, Y. Xu, L. Zhao and N. Huang, *J. Ind. Eng. Chem.*, 2019, **69**, 455–463.
23 A. Inayat, K. Albalawi, A. Rehman, A. Y. Adnan and A. Y. Saad, *Mater. Today Commun.*, 2023, 105479.
24 S. Saini, K. Kumar, P. Saini, D. K. Mahawar, K. S. Rathore, S. Kumar, A. Dandia and V. Parewa, *RSC Adv.*, 2022, **12**(50), 32619–32629.
25 D. K. Dang, C. Sundaram, Y. L. T. Ngo, J. S. Chung, E. J. Kim and S. H. Hur, *Sens. Actuators B Chem.*, 2018, **255**, 3284–3291.
26 Y. Wang, Y. Liu, J. Zhou, J. Yue, M. Xu, B. An, C. Ma, W. Li and S. Liu, *RSC Adv.*, 2021, **11**(47), 29178–29185.

27 H. Xie, Y. Lu, R. You, W. Qian and S. Lin, *RSC Adv.*, 2022, **12**(13), 8160–8171.

28 P. Dubey, K. M. Tripathi, R. Mishra, A. Bhati, A. Singh and S. K. Sonkar, *RSC Adv.*, 2015, **5**(106), 87528–87534.

29 M. J. Molaei, *RSC Adv.*, 2019, **9**(12), 6460–6481.

30 J. R. Bhamore, S. Jha, T. J. Park and S. K. Kailasa, *J. Photochem. Photobiol. B*, 2019, **191**, 150–155.

31 C. J. Jeong, A. K. Roy, S. H. Kim, J. E. Lee, J. H. Jeong, I. In and S. Y. Park, *Nanoscale*, 2014, **6**(24), 15196–15202.

32 H. Diao, T. Li, R. Zhang, Y. Kang, W. Liu and Y. Cui, *Spectrochim. Acta, Part A*, 2018, **200**, 226–234.

33 J. Deng, Y. You, V. Sahajwalla and R. K. Joshi, *Carbon*, 2016, **96**, 105–115.

34 L. Li, G. Wu, G. Yang, J. Peng, J. Zhao and J. Zhu, *Nanoscale*, 2013, **5**(10), 4015–4039.

35 J. Zhang, Y. Yuan, G. Liang and S. Yu, *Adv. Sci.*, 2015, **2**(4), 1500002.

36 Q. Yang, J. Duan, W. Yang, X. Li, J. Mo, P. Yang and Q. Tang, *Appl. Surf. Sci.*, 2018, **434**, 1079–1085.

37 P. Song, L. Zhang, H. Long, M. Meng, T. Liu, Y. Yin and R. Xi, *RSC Adv.*, 2017, **7**(46), 28637–28646.

38 X. Tan, Y. Li, X. Li, S. Zhou, L. Fan and S. Yang, *Chem. Commun.*, 2015, **51**(13), 2544–2546.

39 T. N. J. I. Edison, R. Atchudan, J. J. Shim, S. Kalimuthu, B. C. Ahn and A. R. Lee, *J. Photochem. Photobiol. B*, 2016, **158**, 235–242.

40 D. Sun, R. Ban, P. Zhang, G. Wu, J. Zhang and J. Zhu, *Carbon*, 2013, **64**, 424–434.

41 H. Wang, P. Sun, S. Cong, J. Wu, L. Gao, Y. Wang, X. Dai, Q. Yi and G. Zou, *Nanoscale Res. Lett.*, 2016, **11**, 1–6.

42 H. Ding, X. Zhou, J. Wei, X. Li, B. Qin, X. Chen and H. Xiong, *Carbon*, 2020, **167**, 322–344.

43 X. Yang, Y. Zhuo, S. Zhu, Y. Luo, Y. Feng and Y. Dou, *Biosens. Bioelectron.*, 2014, **60**, 292–298.

44 H. Ding, Y. Ji, J. Wei, Q. Gao, Z. Zhou and H. Xiong, *J. Mater. Chem. B*, 2017, **5**(26), 5272–5277.

45 L. A. Chunduri, A. Kurdekar and S. Patnaik, *Mater. Focus*, 2016, **5**(1), 55–61.

46 X. Jia, J. Li and E. Wang, *Nanoscale*, 2012, **4**(18), 5572–5575.

47 H. Liu, T. Ye and C. Mao, *Angew. Chem., Int. Ed.*, 2007, **119**(34), 6593–6595.

48 J. Shen, Y. Zhu, C. Chen, X. Yang and C. Li, *Chem. Commun.*, 2011, **47**(9), 2580–2582.

49 X. Li, H. Wang, Y. Shimizu, A. Pyatenko, K. Kawaguchi and N. Koshizaki, *Chem. Commun.*, 2010, **47**(3), 932–934.

50 R. Atchudan, T. N. J. I. Edison, S. Perumal, N. C. S. Selvam and Y. R. Lee, *J. Photochem. Photobiol. A*, 2019, **372**, 99–107.

51 J. E. Gill, *Photochem. Photobiol.*, 1969, **9**(4), 313–322.

52 S. Chandra, S. H. Pathan, S. Mitra, B. H. Modha, A. Goswami and P. Pramanik, *RSC Adv.*, 2012, **2**(9), 3602–3606.

53 M. J. Molaei, *Anal. Methods*, 2020, **12**(10), 1266–1287.

54 T. Gokus, R. R. Nair, A. Bonetti, M. Bohmler, A. Lombardo, K. S. Novoselov, A. K. Geim, A. C. Ferrari and A. Hartschuh, *ACS Nano*, 2009, **3**(12), 3963–3968.

55 X. Meng, Q. Chang, C. Xue, J. Yang and S. Hu, *Chem. Commun.*, 2017, **53**(21), 3074–3077.

56 L. Wang, W. Li, L. Yin, Y. Liu, H. Guo, J. Lai and Y. Han, *Sci. Adv.*, 2020, **6**(40), eabb6772.

57 D. Shen, Y. Long, J. Wang, Y. Yu, J. Pi, L. Yang and H. Zheng, *Nanoscale*, 2019, **11**(13), 5998–6003.

58 H. Ding, S. Yu, J. Wei and H. Xiong, *ACS Nano*, 2016, **10**(1), 484–491.

59 L. Bao, Z. Zhang, Z. Tian, L. Zhang, C. Liu, Y. Lin, B. Qi and D. Pang, *Adv. Mater.*, 2011, **23**(48), 5801–5806.

60 V. Nguyen, J. Si, L. Yan and X. Hou, *Carbon*, 2016, **108**, 268–273.

61 Y. Zhang, R. Yuan, M. He, G. Hu, J. Jiang, T. Xu and L. Zhou, *Nanoscale*, 2017, **9**(45), 17849–17858.

62 J. B. Essner, J. A. Kist, L. Polo-Parada and G. A. Baker, *Chem. Mater.*, 2018, **30**(6), 1878–1887.

63 J. Schneider, C. J. Reckmeier, Y. Xiong, M. V. Seckendorff, A. S. Susha, P. Kasak and A. L. Rogach, *J. Phys. Chem. C*, 2017, **121**(3), 2014–2022.

64 M. J. Krysmann, A. Kelarakis, P. Dallas and E. P. Giannelis, *J. Am. Chem. Soc.*, 2012, **134**(2), 747–750.

65 S. Zhu, Q. Meng, L. Wang, J. Zhang, Y. Song, H. Jin and K. Zhang, *Angew. Chem., Int. Ed.*, 2013, **52**(14), 3953–3957.

66 P. Yu, X. Wen, Y. R. Toh and J. Tang, *J. Phys. Chem. C*, 2012, **116**(48), 25552–25557.

67 S. Sun, L. Zhang, K. Jiang, A. Wu and H. Lin, *Chem. Mater.*, 2016, **28**(23), 8659–8668.

68 S. Qu, D. Zhou, D. Li, W. Ji, P. Jing, D. Han, L. Liu, H. Zeng and D. Shen, *Adv. Mater.*, 2016, **28**(18), 3516–3521.

69 S. K. Kailasa, S. Ha, S. H. Baek, L. M. T. Phan, S. Kim, K. Kwak and T. J. Park, *Mater. Sci. Eng. C*, 2019, **98**, 834–842.

70 L. Li, R. Zhang, C. Lu, J. Sun and L. Wang, *J. Mater. Chem. B*, 2017, **5**(35), 7328–7334.

71 Y. Zhou, Y. Liu, Y. Li, Z. He, Q. Xu, Y. Chen, J. Street, H. Guo and M. Nelles, *RSC Adv.*, 2018, **8**(42), 23657–23662.

72 X. Gong, W. Lu, Y. Liu, Z. Li, S. Shuang, C. Dong and M. M. F. Choi, *J. Mater. Chem. B*, 2015, **3**(33), 6813–6819.

73 P. Das, S. Ganguly, P. P. Maity, M. Bose, S. Mondal and S. Dhara, *J. Photochem. Photobiol. B*, 2018, **180**, 56–67.

74 Y. Wang and A. Hu, *J. Mater. Chem. C*, 2014, **2**(34), 6921–6939.

75 L. Cao, X. Wang, M. J. Meziani, F. S. Lu, H. F. Wang and P. J. G. Luo, *J. Am. Chem. Soc.*, 2007, **129**(37), 11318–11319.

76 B. Yin, J. Deng, X. Peng, Q. Long, J. Zhao, Q. Lu and Q. Chen, *Analyst*, 2013, **138**(21), 6551–6557.

77 C. Jiang, H. Wu, X. Song, X. Ma, J. Wang and M. Tan, *Talanta*, 2014, **127**, 68–74.

78 X. Wen, P. Yu, Y. R. Toh, X. Ma and J. Tang, *Chem. Commun.*, 2014, **50**(36), 4703–4706.

79 Y. Song, S. Zhu and B. Yang, *RSC Adv.*, 2014, **4**(52), 27184–27200.

80 S. Dadkhah, A. Mehdinia, A. Jabbari and A. Manbohi, *Microchim. Acta*, 2020, **187**(10), 1–12.

81 M. Mahani, Z. Mousapour, F. Divsar, A. Nomani and H. Ju, *Microchim. Acta*, 2019, **186**(3), 1–8.

82 K. Dehvari, K. Liu, P. J. Tseng, G. Gedda, W. M. Girma and J. Chang, *J. Taiwan Inst. Chem. Eng.*, 2019, **95**, 495–503.

83 H. Miao, L. Wang, Y. Zhuo, Z. Zhou and X. Yang, *Biosens. Bioelectron.*, 2016, **86**, 83–89.

84 A. Prasannan and T. Imae, *Ind. Eng. Chem. Res.*, 2013, **52**(44), 15673–15678.

85 K. Qi, M. Song, X. Xie, Y. Wen, Z. Wang, B. Wei and Z. Wang, *Chemosphere*, 2021, 132192.

86 S. Jing, Y. Zhao, R. Sun, L. Zhong and X. Peng, *ACS Sustain. Chem. Eng.*, 2019, 7, 7833–7843.

87 C. Wang, H. Shi, M. Yang, Y. Yan, E. Liu, Z. Ji and J. Fan, *Mater. Res. Bull.*, 2020, **124**(Apr), 110730.

88 V. C. Hoang, L. H. Nguyen and V. G. Gomes, *J. Electroanal. Chem.*, 2019, **832**, 87–96.

89 P. Huang, S. Xu, M. Zhang, W. Zhong, Z. Xiao and Y. Luo, *Opt. Mater.*, 2020, **110**(2), 110535.

90 J. Zhou, Z. Sheng, H. Han, M. Zou and C. Li, *Mater. Lett.*, 2012, **66**(1), 222–224.

91 M. Xue, Z. Zhan, M. Zou, L. Zhang and S. Zhao, *New J. Chem.*, 2016, **40**(2), 1698–1703.

92 X. Tan, A. N. B. Romainor, S. F. Chin and S. M. Ng, *J. Anal. Appl. Pyrol.*, 2014, **105**, 157–165.

93 X. Ma, Y. Dong, H. Sun and N. Chen, *Mater. Today Chem.*, 2017, **5**, 1–10.

94 S. K. Bajpai, A. D'souza and B. Suhail, *Int. Nano Lett.*, 2019, **9**, 203–212.

95 Q. Huang, Q. Li, Y. Chen, L. Tong, X. Lin, J. Zhu and Q. Tong, *Sens. Actuators B Chem.*, 2018, **276**, 82–88.

96 M. Si, J. Zhang, Y. He, Z. Yang, X. Yan, M. Liu and S. Zhuo, *Green Chem.*, 2018, **20**(15), 3414–3419.

97 C. Zhao, X. Li, C. Cheng and Y. Yang, *Microchem. J.*, 2019, **147**, 183–190.

98 N. Arsalani, P. Nezhad-Mokhtari and E. Jabbari, *Artif. Cell Nanomed. Biotechnol.*, 2019, **47**(1), 540–547.

99 Z. Wei, B. Wang, Y. Liu, Z. Liu, H. Zhang, S. Zhang, J. Chang and S. Lu, *New J. Chem.*, 2019, **43**(2), 718–723.

100 H. Miao, Y. Wang and X. Yang, *Nanoscale*, 2018, **10**(17), 8139–8145.

101 G. Wang, Q. Guo, D. Chen, Z. Liu, X. Zheng, A. Xu, S. Yang and G. Ding, *ACS Appl. Mater. Interfaces*, 2018, **10**(6), 5750–5759.

102 G. Chellasamy, S. K. Arumugasamy, S. Govindaraju and K. Yun, *Chemosphere*, 2022, **287**, 131915.

103 L. Ge, H. Yu, H. Ren, B. Shi, Q. Guo, W. Gao, Z. Li and J. Li, *J. Mater. Sci.*, 2017, **52**(17), 9979–9989.

104 F. Yuan, Z. Wang, X. Li, Y. Li, Z. Tan, L. Fan and S. Yang, *Adv. Mater.*, 2017, **29**(3), 1604436.

105 W. Liu, C. Li, Y. Ren, X. Sun, W. Pan, Y. Li, J. Wang and W. Wang, *J. Mater. Chem. B*, 2016, **4**(35), 5772–5788.

106 J. Zhou, H. Zhou, J. Tang, S. Deng, F. Yan, W. Li and M. Qu, *Microchim. Acta*, 2017, **184**, 343–368.

107 M. A. Sk, A. Ananthanarayanan, L. Huang, K. Lim and P. Chen, *J. Mater. Chem. C*, 2014, **2**(34), 6954–6960.

108 S. Miao, K. Liang, J. Zhu, B. Yang, D. Zhao and B. Kong, *Nano Today*, 2020, **33**, 100879.

109 F. Li, D. Yang and H. Xu, *Chem. –Eur. J.*, 2019, **25**(5), 1165–1176.

110 H. Huang, J. Lv, D. Zhou, N. Bao, Y. Xu, A. Wang and J. Feng, *RSC Adv.*, 2013, **3**(44), 21691–21696.

111 L. Li and T. Dong, *J. Mater. Chem. C*, 2018, **6**(30), 7944–7970.

112 X. Gong, W. Lu, M. C. Paau, Q. Hu, X. Wu, S. Shuang, C. Dong and M. M. F. Choi, *Anal. Chim. Acta*, 2015, **861**, 74–84.

113 Y. Zhang, X. Liu, Y. Fan, X. Guo, L. Zhou, Y. Lv and J. Lin, *Nanoscale*, 2016, **8**(33), 15281–15287.

114 H. Liu, Z. Li, Y. Sun, X. Geng, Y. Hu, H. Meng, J. Ge and L. Qu, *Sci. Rep.*, 2018, **8**(1), 1086.

115 D. Qu, M. Zheng, L. Zhang, H. Zhao, Z. Xie, X. Jing, R. E. Haddad, H. Fan and Z. Sun, *Sci. Rep.*, 2014, **4**(1), 1–11.

116 J. Ju and W. Chen, *Biosens. Bioelectron.*, 2014, **58**, 219–225.

117 S. Do, W. Kwon, Y. H. Kim, S. R. Kang, T. Lee, T. W. Lee and S. W. Rhee, *Adv. Opt. Mater.*, 2016, **4**(2), 276–284.

118 X. Shan, L. Chai, J. Ma, Z. Qian, J. Chen and H. Feng, *Analyst*, 2014, **139**(10), 2322–2325.

119 J. Zhou, X. Shan, J. Ma, Y. Gu, Z. Qian, J. Chen and H. Feng, *RSC Adv.*, 2014, **4**(11), 5465–5468.

120 Q. Ye, F. Yan, Y. Luo, Y. Wang, X. Zhou and L. Chen, *Spectrochim. Acta, Part A*, 2017, **173**, 854–862.

121 L. Tan, G. Huang, T. Liu, C. Fu, Y. Zhou, Z. Zhu and X. Meng, *J. Nanosci. Nanotechnol.*, 2016, **16**(3), 2652–2657.

122 G. Zuo, A. Xie, J. Li, T. Su, X. Pan and W. Dong, *J. Phys. Chem. C*, 2017, **121**(47), 26558–26565.

123 A. Cayuela, M. L. Soriano, S. R. Kennedy, J. W. Steed and M. Valcarcel, *Talanta*, 2016, **151**, 100–105.

124 S. Bhatt, M. Bhatt, A. Kumar, G. Vyas, T. Gajaria and P. Paul, *Colloids Surf., B*, 2018, **167**, 126–133.

125 Y. Liu, Y. Zhao and Y. Zhang, *Sens. Actuators B Chem.*, 2014, **196**, 647–652.

126 X. Fang, M. Li, K. Guo, J. Li, M. Pan, L. Bai, M. D. Luoshan and X. Zhao, *Electrochim. Acta*, 2014, **137**, 634–638.

127 X. Sun and Y. Lei, *TrAC, Trends Anal. Chem.*, 2017, **89**, 163–180.

128 H. Huang, H. Ge, Z. Ren, Z. Huang, M. Xu and X. Wang, *Front. Bioeng. Biotechnol.*, 2021, **9**, 617097.

129 Y. Zhang, L. Wang, H. Zhang, Y. Liu, H. Wang, Z. Kang and S. T. Lee, *RSC Adv.*, 2013, **3**(11), 3733–3738.

130 Z. Xie, X. Sun, J. Jiao and X. Xin, *Colloids Surf., A*, 2017, **529**, 38–44.

131 W. Li, S. Huang, H. Wen, Y. Luo, J. Cheng, Z. Jia, P. Han and W. Xue, *Anal. Bioanal. Chem.*, 2020, **412**, 993–1002.

132 A. Tadesse, M. Hagos, D. RamaDevi, N. Belachew and K. Basavaiah, *ACS Omega*, 2020, **5**(8), 3889–3898.

133 J. Mu, J. Yang, D. Zhang and Q. Jia, *Chin. J. Anal. Chem.*, 2021, **49**(3), 319–329.

134 Y. Huang, Y. Zhang, F. Huo, Y. Wen and C. Yin, *Sci. China Chem.*, 2020, **63**, 1742–1755.

135 X. Wu, C. Ma, J. Liu, Y. Liu, S. Luo and M. Xu, *Microchem. J.*, 2019, **7**(23), 18801–18809.

136 Y. Duan, Z. Li, X. Liu, H. Pang, L. Huang, X. Sun and Y. Shi, *J. Alloys Compd.*, 2022, **921**, 166088.

137 L. Yang, F. Zhu, H. Tan, F. Wang and Z. Wang, *Packag. Jpn.*, 2021, **13**(5), 16–26.

138 X. Yu, X. Chen, B. Zhang, C. Rao, Y. He and J. Li, *Prog. Chem.*, 2016, **28**(6), 896–907.

139 W. Du, X. Xu, H. Hao, R. Liu, D. Zhang, F. Gao and Q. Lu, *Sci. China Chem.*, 2015, **58**, 863–870.

140 W. Liu, H. Diao, H. Chang, H. Wang, T. Li and W. Wei, *Sens. Actuators B Chem.*, 2017, **241**, 190–198.

141 J. Yu, N. Song, Y. Zhang, S. Zhong, A. Wang and J. Chen, *Sens. Actuators B Chem.*, 2015, **214**, 29–35.

142 L. Li, L. Shi, J. Jia, D. Chang, C. Dong and S. Shuang, *Analyst*, 2020, **145**(16), 5450–5457.

143 R. Atchudan, T. N. J. I. Edison, K. R. Aseer, S. Perumal, N. Karthik and Y. R. Lee, *Biosens. Bioelectron.*, 2018, **99**, 303–311.

144 Y. Zhang, K. F. Chan, B. Wang, P. W. Y. Chiu and L. Zhang, *Sens. Actuators B Chem.*, 2018, **271**, 128–136.

145 J. Shen, S. Shang, X. Chen, D. Wang and Y. Cai, *Mater. Sci. Eng. C*, 2017, **76**, 856–864.

146 S. Zhao, X. Song, X. Chai, P. Zhao, H. He and Z. Liu, *J. Clean. Prod.*, 2020, **263**, 121561.

147 U. Latief, S. A. Islam, Z. M. S. H. Khan and M. S. Khan, *Spectrochim. Acta, Part A*, 2021, **262**, 120132.

148 S. Venkateswarlu, B. Viswanath, A. S. Reddy and M. Yoon, *Sens. Actuators B Chem.*, 2018, **258**, 172–183.

149 N. Pourreza and M. Ghomi, *Mater. Sci. Eng., C*, 2019, **98**, 887–896.

150 Z. Ye, Y. Zhang, G. Li and B. Li, *Anal. Lett.*, 2020, **53**(18), 2841–2853.

151 Z. Gao, Z. Lin, X. Chen, Z. Lai and Z. Huang, *Sens. Actuators B Chem.*, 2016, **222**(JAN), 965–971.

152 J. Praneerad, N. Thongsai, P. Supchocksoonthorn, S. Kladsomboon and P. Paoprasert, *Spectrochim. Acta Mol. Biomol. Spectrosc.*, 2019, **211**, 59–70.

153 J. R. Bhamore, S. Jha, T. J. Park and S. K. Kailasa, *Sens. Actuators B Chem.*, 2018, **277**, 47–54.

154 J. Xu, C. Wang, H. Li and W. Zhao, *RSC Adv.*, 2020, **10**(5), 2536–2544.

155 N. Chaudhary, P. K. Gupta, S. Eremin and P. R. Solanki, *J. Environ. Chem. Eng.*, 2020, **8**(3), 103720.

156 N. Murugan, M. Prakash, M. Jayakumar, A. Sundaramurthy and A. K. Sundramoorthy, *Appl. Surf. Sci.*, 2019, **476**, 468–480.

157 J. Li, O. Xu and X. Zhu, *RSC Adv.*, 2021, **11**(54), 34107–34116.

158 B. Rooj, A. Dutta, S. Islam and U. Mandal, *J. Fluoresc.*, 2018, **28**, 1261–1267.

159 L. Wang, W. Li, B. Wu, Z. Li, S. Wang, Y. Liu, D. Pan and M. Wu, *Chem. Eng. J.*, 2016, **300**, 75–82.

160 R. Bandi, R. Dadigala, B. R. Gangapuram and V. Guttena, *J. Photochem. Photobiol., B*, 2018, **178**, 330–338.

161 B. T. Hoan, T. T. Thanh, P. D. Tam, N. N. Trung, S. Cho and V. Pham, *Mater. Sci. Eng., B*, 2019, **251**, 114455.

162 J. R. Bhamore, S. Jha, R. K. Singhal, T. Park and S. K. Kailasa, *J. Mol. Liq.*, 2018, **264**, 9–16.

163 X. Wen, L. Shi, G. Wen, Y. Li, C. Dong, J. Yang and S. Shuang, *Sens. Actuators B Chem.*, 2016, **235**, 179–187.

164 B. Luo, H. Yang, B. Zhou, S. M. Ahmed, Y. Zhang, H. Liu, X. Liu, Y. He and S. Xia, *ACS Omega*, 2020, **5**(10), 5540–5547.

165 K. Rajendran and N. Rajendiran, *Mater. Res. Express*, 2018, **5**(2), 024008.

166 F. Cai, X. Liu, S. Liu, H. Liu and Y. Huang, *RSC Adv.*, 2014, **4**(94), 52016–52022.

167 Y. Liu, J. Hu, Y. Li, H. Wei, X. Li, X. Zhang, S. Chen and X. Chen, *Talanta*, 2015, **134**, 16–23.

168 A. Tyagi, K. M. Tripathi, N. Singh, S. Choudhary and R. K. Gupta, *RSC Adv.*, 2016, **6**(76), 72423–72432.

169 H. Fan, M. Zhang, B. Bhandari and C. Yang, *Trends Food Sci. Technol.*, 2020, **95**, 86–96.

170 D. Dang, C. Sundaram, Y. L. T. Ngo, W. M. Choi, J. S. Chung, E. J. Kim and S. H. Hui, *Dyes Pigments*, 2019, **165**, 327–334.

171 N. Amin, A. Afkhami, L. Hosseinzadeh and T. Madrakian, *Anal. Chim. Acta*, 2018, **1030**, 183–193.

172 Y. K. Gun'ko, *Nanomaterials*, 2016, **6**(6), 105.

173 K. Shivaji, S. Mani, P. Ponmurugan, C. S. D. Castro, M. L. Davies, M. G. Balasubramanian and S. Pitchaimuthu, *ACS Appl. Nano Mater.*, 2018, **1**(4), 1683–1693.

174 J. Liu, Y. Geng, D. Li, H. Yao, Z. Huo, Y. Li, K. Zhang, S. Zhu, H. Wei, W. Xu, J. Jiang and B. Yang, *Adv. Mater.*, 2020, **32**(17), 1906641.

175 Y. Li, G. Bai, S. Zeng and J. Hao, *ACS Appl. Mater. Interfaces*, 2019, **11**(5), 4737–4744.

176 B. Chen, F. Li, S. Li, W. Weng, H. Guo, T. Guo, X. Zhang, Y. Chen and T. Huang, *Nanoscale*, 2013, **5**(5), 1967–1971.

177 L. Shi, Y. Li, X. Li, X. Wen, G. Zhang, J. Yang, C. Dong and S. Shuang, *Nanoscale*, 2015, **7**(16), 7394–7401.

178 R. Rani, V. Kumar and F. Rizzolio, *ACS Med. Chem. Lett.*, 2018, **9**(1), 4–5.

179 V. N. Mehta, S. S. Chettiar, J. R. Bhamore, S. K. Kailasa and R. M. Patel, *J. Fluoresc.*, 2017, **27**, 111–124.

180 K. Dehvari, K. Liu, P. J. Tseng, G. Gedda, W. M. Girma and J. Chang, *J. Taiwan Inst. Chem. Eng.*, 2019, **95**, 495–503.

181 S. L. D'souza, B. Deshmukh, J. R. Bhamore, K. A. Rawat, N. Lenka and S. K. Kailasa, *RSC Adv.*, 2016, **6**(15), 12169–12179.

182 S. Ahmadian-Fard-Fini, M. Salavati-Niasari and D. Ghanbari, *Spectrochim. Acta, Part A*, 2018, **203**, 481–493.

183 T. S. John, P. K. Yadav, D. Kumar, S. K. Singh and S. H. Hasan, *Luminescence*, 2020, **35**(6), 913–923.

184 M. I. Kim, S. Y. Park, K. S. Park, S. R. Kim, J. P. Kim, Y. C. Lee, H. U. Lee and H. G. Park, *Sens. Actuators, B*, 2018, **262**, 469–476.

185 K. D. J. Gracia, S. S. Thavamani, T. P. Amaladhas, S. Devanesan, M. Ahmed and M. M. Kannan, *Chemosphere*, 2022, **298**, 134128.

186 S. Pramanik, S. Chatterjee, G. S. Kumar and P. S. Devi, *Phys. Chem. Chem. Phys.*, 2018, **20**(31), 20476–20488.

187 S. Godavarthi, K. M. Kumar, E. V. Velez, A. Hernandez-Eligio and M. Mahendhiran, *J. Photochem. Photobiol. B*, 2017, **172**, 36–41.

188 B. Kumari, R. Kumari and P. Das, *J. Pharm. Biomed. Anal.*, 2018, **157**, 137–144.

189 W. Meng, X. Bai, B. Wang, Z. Liu, S. Lu and B. Yang, *Energy Environ. Mater.*, 2019, **2**(3), 172–192.

190 J. Zhu, J. Roscow, S. Chandrasekaran, L. Deng, P. Zhang, T. He, K. Wang and L. Huang, *ChemSusChem*, 2020, **13**(6), 1275–1295.

191 Y. Li, Y. Hu, Y. Zhao, G. Shi, L. Deng, Y. Hou and L. Qu, *Adv. Mater.*, 2011, **23**(6), 776–780.

192 X. Wang, L. Xu, S. Ge, S. Y. Foong, R. K. Liew and W. W. F. Chong, *Energy*, 2023, **274**, 127354.

193 A. Marinovic, L. S. Kiat, S. Dunn, M. M. Titirici and J. Briscoe, *ChemSusChem*, 2017, **10**(5), 1004–1013.

194 Y. Meng, Y. Zhang, W. Sun, M. Wang, B. He, H. Chen and Q. Tang, *Electrochim. Acta*, 2017, **257**, 259–266.

195 L. Liu, X. Yu, Z. Yi, F. Chi, H. Wang, Y. Yuan, D. Li, K. Xu and X. Zhang, *Nanoscale*, 2019, **11**(32), 15083–15090.

196 M. R. Pacquiao, M. D. G. D. Luna, N. Thongsai, S. Kladsomboon and P. Paoprasert, *Appl. Surf. Sci.*, 2018, **453**, 192–203.

197 M. Xu, Q. Huang, R. Sun and X. Wang, *RSC Adv.*, 2016, **6**(91), 88674–88682.